



LIBRARY
Michigan State
University

This is to certify that the

thesis entitled

A BRUSHLESS DIRECT CURRENT MOTOR DRIVE WITHOUT ROTOR POSITION SENSORS

presented by

Michael Paul Copeland

has been accepted towards fulfillment of the requirements for

Master's degree in Electrical Eng.

Major professor

Date 1 May 97

O-7639

MSU is an Affirmative Action/Equal Opportunity Institution

PLACE IN RETURN BOX to remove this checkout from your record.

TO AVOID FINES return on or before date due.

DATE DUE	DATE DUE	DATE DUE

MSU is An Affirmative Action/Equal Opportunity Institution

A BRUSHLESS DIRECT CURRENT MOTOR DRIVE WITHOUT ROTOR POSITION SENSORS

By

Michael Paul Copeland

A THESIS

Submitted to
Michigan State University
in partial fulfillment of the requirements
for the degree of

MASTER OF SCIENCE

Department of Electrical Engineering

1997

ABSTRACT

A BRUSHLESS DIRECT CURRENT MOTOR DRIVE WITHOUT ROTOR POSITION SENSORS

By

Michael Paul Copeland

A drive which enables sensorless operation of brushless direct current motors with trapezoidal flux distributions is proposed. The proposed drive improves upon an older version but is implemented using different hardware and a microcontroller for greater flexibility. The microcontroller allows easy implementation of more sophisticated control schemes which result in extending the speed range of the motor. Experimental results show that the proposed operating scheme without modification allows the motor to be operated at speeds as low as 55 rpm and higher than 2500 rpm with reasonable dynamic performance. More sophisticated control schemes can only improve these results.

ACKNOWLEDGMENTS

The work contained herein would not have been possible without the guidance of Dr.

Elias Strangas and the support of the students of the Electrical Machines Lab at Michigan

State University.

TABLE OF CONTENTS

IST OF FIGURES	
CHAPTER 1	
INTRODUCTION	1
Structure and Operation of BLDC Motors	
Reasons to Eliminate Rotor Position Sensors	
Challenges of Sensorless Operation	
CHAPTER 2	
METHODS OF SENSORLESS OPERATION	10
Estimator Based Position Detection	10
Discrete Position Detection	11
Zero Crossing Detection Method	12
Ogasawara and Akagi's Method	
Disadvantages Of Ogasawara and Akagi's Method	
Difficulty in Maximizing Motor Operating Speed Range	
Problems with Dynamic Performance	
CHAPTER 3	
MODIFICATIONS TO OGASAWARA AND AKAGI'S METHOD	28
Proposed Improvements	
Proposed Sensorless Operating Scheme	33
CHAPTER 4	
EXPERIMENTAL SETUP	37
Chopping Selector Circuit	
Detection Circuit.	
Inverter	
Brushless DC Motor	
Microcontroller	
MICIOCOMUONET	43

CHAPTER 5	
DESCRIPTION OF EXPERIMENTS AND RESULTS	
Determination of Constants	
Tuning and Validation of the Detection Circuit	•••••
Determination of K _c	•••••
Validation of Chopping Reduction and Chopping Frequen	
OTT I DOTTE C	
CHAPTER 6	
FUTURE IMPROVEMENTS	
Dynamic Load Compensation	
Elimination Of Chopping	•••••
CHAPTER 7	
CONCLUSIONS AND COMMENTS	••••••
APPENDIX A	
	••••••
BIBLIOGRAPHY	•••••

LIST OF FIGURES

Figure 1.1 - BLDC Motor	3
Figure 1.2 - Developed Torque	4
Figure 1.3 - BLDC Motor with Hall-Effect Sensors	
Figure 2.1 - Line-to-Neutral Back EMF and Corresponding Switching Events	13
Figure 2.2 - Inverter and Motor with A+ and B- Conducting	
Figure 2.3 - Inverter and Motor with D _{B+} and A+ Conducting	17
Figure 2.4 - Line-to-Neutral Back EMF and Switching Events Including Chopping	19
Figure 2.5 - Detection Circuit Using Floating DC Supplies	
Figure 2.6 - Motor Cross Section During Initialization of Starting Procedure	22
Figure 2.7 - Motor Cross Section During Second Phase of Starting Procedure	23
Figure 2.8 - Detection Error at High Speeds	25
Figure 2.9 - Detection Error at Low Speeds	26
Figure 3.1 - Detection Circuit Implemented with Current Transducers	
Figure 3.2 - Waveforms of the Current Detection Circuit	31
Figure 3.3 - Proposed System for Sensorless Operation	33
Figure 3.4 - Simple Method of Commutation Time Prediction	34
Figure 3.5 - Preferred Method of Determining Commutation Time	35
Figure 4.1 - Chopping Selector Circuit	38
Figure 4.2 - Detection Circuit	
Figure 4.3 - Flow Chart of Main Program and ITC ISR	47
Figure 4.4 - Flow Chart of Output Compare ISR	
Figure 5.1 - A+ When the Motor is Operating Properly	51
Figure 5.2 - A+ When Detection Circuit is Unbalanced	52
Figure 5.3 - Phase Current and Its Detection	53
Figure 5.4 - Phase Current When K _c is too Large	54
Figure 5.5 - Phase Current When K _c is too Small	55
Figure 5.6 - Phase Current For Proper K _c	55
Figure 5.7 - Low Speed Error Correction	56
Figure 6.1 - Algorithm for Dynamic Load Compensation	61

Chapter 1

INTRODUCTION

Brushless direct current (BLDC) motors are used in a wide variety of applications due to their ruggedness, torque to volume ratio, and linear control characteristics. These motors require rotor position sensors for reliable operation. The possibility of eliminating position sensors has been investigated for some time. This thesis describes the theory behind several rotor position detection methods and the implementation of one method in more flexible hardware. Also discussed are some of the possible enhancements which could be implemented with this new hardware.

1.1 STRUCTURE AND OPERATION OF BLDC MOTORS

BLDC motors have permanent magnets fixed to the rotor and stator windings which are either sinusoidally distributed or rectangular. The method of operation is very different for the two different types of motors. If the stator windings are sinusoidally distributed, then as the rotor spins it will induce a sinusoidal voltage in the stator. If the stator has rectangular windings the induced voltage (back emf) will be trapezoidal. The nearly trapezoidal shape of the back emf is a property that will be exploited in this thesis.

This thesis concentrates on three phase wye connected BLDC motors that have trapezoidal induced voltages and permanent magnets that cover the entire rotor circumference. Throughout this thesis, BLDC motors with sinusoidally distributed back emf will be called sinusoidal BLDC and motors with trapezoidal back emf and rotor magnets that cover the entire rotor circumference will be called trapezoidal BLDC.

BLDC motors with rotor magnets that do not cover the entire rotor circumference are not discussed here.

Figure 1.1 shows the wye connection of the three motor phases and a cross section of a two pole motor. The outer ring of the motor represents the stator, and the inner circle represents the permanent magnet rotor. Each of the three stator windings, labeled A, B, and C (one for each phase), cover 120° of the stator. The stator is wound so that when the section of the winding labeled B carries current that directed out of the paper, the section labeled B' carries current that is directed into the paper.

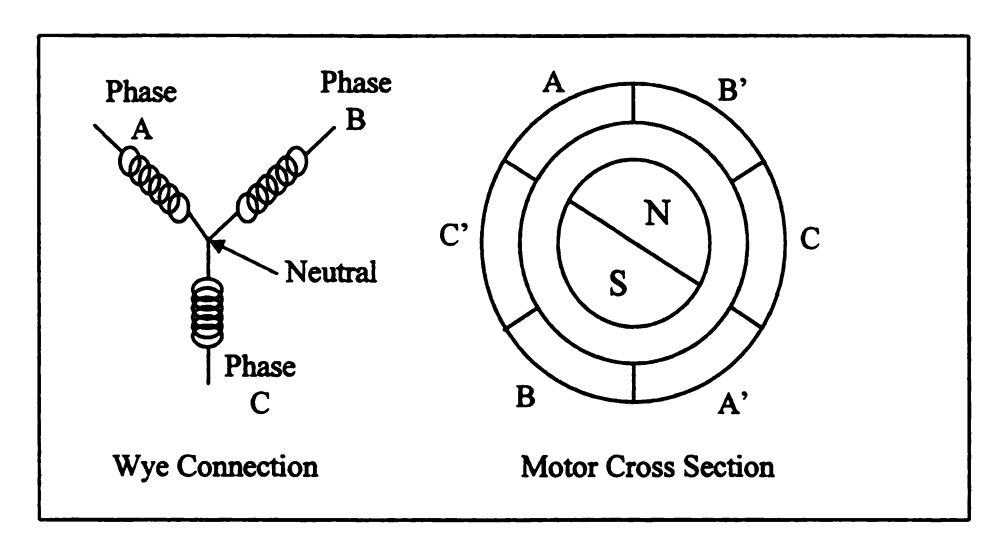


Figure 1.1 - BLDC Motor

To achieve the maximum torque the rotor poles should be aligned with the stator windings that are conducting current, as shown in Figure 1.2. The torque is then caused by the Lorentz force ($B \times i$) that occurs when the current of the stator interacts with the flux density of the rotor magnets, as shown in Figure 1.2. Figure 1.2 shows the cross section of the motor when phases B and C are conducting and phase A is not conducting. Current out of the paper is indicated by the small circles that contain dots, while current into the paper is represented by the small circles that contain crosses. The developed torque is represented by the arrows in the motor air gap.

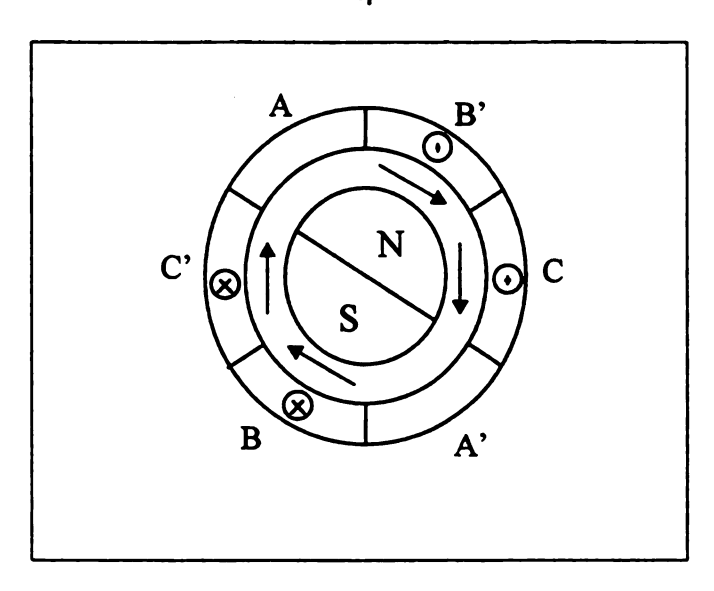


Figure 1.2 - Developed Torque

Notice that as the rotor turns in the direction of the developed torque, the maximum torque will continue to be developed for the next sixty degrees of rotation.

After sixty degrees, the rotor will be in the position indicated by Figure 1.3. At this point, if the motor is to continue developing maximum torque, phase B must stop conducting and phase A must start conducting (as shown in Figure 1.3). This event is referred to as a commutation.

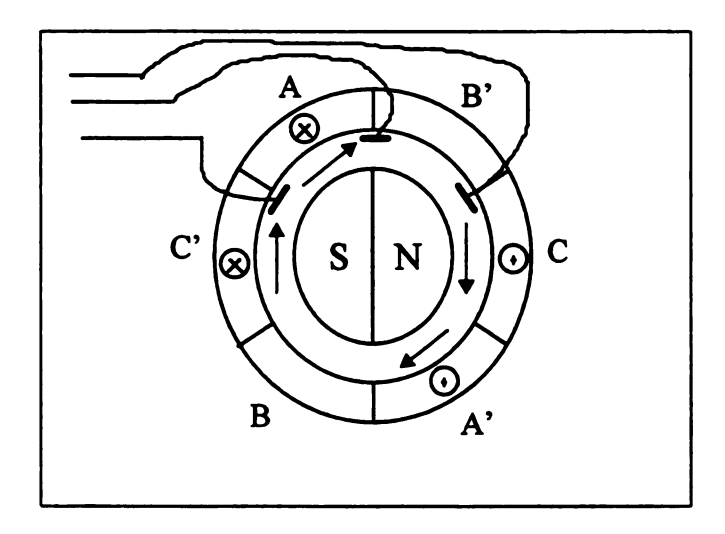


Figure 1.3 - BLDC Motor with Hall-Effect Sensors

Since the commutation depends on the position of the rotor, an encoder or Hall-effect sensors (sensors which indicate which rotor pole is closest) can be used to determine the proper time for the commutation. Figure 1.3 also shows where Hall-effect sensors are normally placed in the stator.

The motor is generally fed by a three phase inverter which consists of the usual six power transistors each equipped with a body or free-wheeling diode for protection as shown in Figure 1.4. The DC voltage that is applied to the motor is usually increased or decreased by simply chopping (turning off) one of the inverter transistors at a fixed frequency with a varying duty cycle. Speed or torque is then controlled by increasing or decreasing the duty cycle which respectively increases or decreases the applied DC voltage.

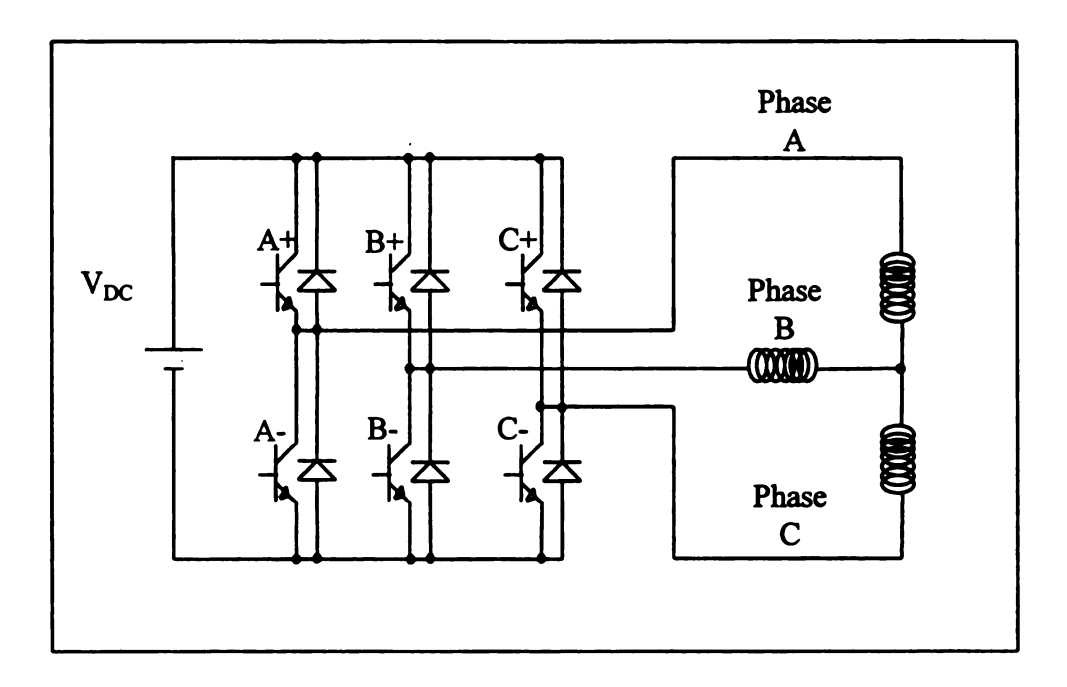


Figure 1.4 - Inverter with BLDC Motor Load

It should be noted that for the remainder of this thesis positive current will be defined as current directed into the motor (or out of the inverter) and negative current is current that is directed out of the motor (or into the inverter). So, for example, if it is desired that phase A carry positive current and phase B carry negative current, the transistors labeled "A+" and "B-" must be forced to conduct. This will result in V_{DC} being applied to the motor terminals. If only 25% of the value of V_{DC} is desired, then either transistor A+, or B- (or both) must be turned off (chopped) 75% of the time. This implies that a 25% duty cycle should be used for chopping.

1.2 REASONS TO ELIMINATE ROTOR POSITION SENSORS

There are essentially two "universal" incentives for eliminating rotor position sensors. The first incentive is that rotor position sensors are a very common source of failure in a BLDC motor. Therefore, their elimination would extend the useful life of the motor. The other reason to remove rotor position sensors is that it requires extra steps in the manufacturing process to add sensors to the motor. Therefore BLDC motors can be manufactured less expensively if the sensors are removed. Although removing the sensors requires extra control circuitry, this circuitry is external to the motor, and is easily mass produced and less expensive to replace in the event of a failure.

In addition to these "universal" benefits of removing rotor position sensors, there are several specific applications in which sensors are not desired. As described in [1], BLDC motors are often used in compressors and must be enclosed by a hermetic alloy. This requires seals around all of the wires that connect the motor to the controller. Removing the rotor position sensors will significantly decrease the number of wires going to the motor and thus reduce the number of hermetic seals.

Sensorless BLDC motors are also desirable in environments where extra wires effect the electro-magnetic interference (EMI) properties of the system. Sensorless motors are very attractive for automotive applications since the EMI properties of an automobile can be significantly effected by the number and length of wires that are contained in the vehicle.

1.3 CHALLENGES OF SENSORLESS OPERATION

All sensorless operating schemes for BLDC motors rely on either detecting, calculating or estimating the voltage that is induced in the stator by the moving rotor. The rotor position can then be determined since the induced voltage has either a trapezoidal or sinusoidal shape (with respect to the rotor position). This detection or calculation is done by examining the phase currents and voltages. The problem is that the back emf is very small at low rotor speeds and thus difficult to calculate. Of course there is no back emf when the rotor is not moving. This makes starting the motor a challenge. Most sensorless operating schemes require the motor to be operated in an open loop mode until the rotor spins fast enough for the back emf to become detectable.

Open loop starting procedures have several draw backs. The most obvious of these is that the motor has no way of controlling acceleration or torque unless the load is known. This makes open loop schemes susceptible to stalls and/or large torque ripple. If the open loop starting procedure is too long, then the number of applications where the sensorless operating method will be useful can become limited.

Another drawback to any open loop starting scheme is that the first time any phase coil is energized, the rotor will move either forward or backward. The direction of initial movement is determined by the initial rotor position which is unknown prior to starting. Even if the open loop starting scheme lasts only one commutation, the rotor will always have the possibility of momentarily moving backwards. This too may limit the number of applications where an open loop starting procedure can be used.

Yet another problem with open loop starting schemes is that they can be very inefficient since there is no way to ensure that the rotor poles are aligned properly with the energized coils. If the proper stator windings are not energized at the proper times, the rotor will draw more current than is needed. Since an open loop starting procedure is required, a challenge of any sensorless operating scheme is to make that procedure as short as possible.

Maximizing the motors speed range is also difficult for sensorless drives. As mentioned before, the induced voltage is very difficult to calculate at low rotor speeds.

As will be shown in chapter 2, high rotor speeds can also present problems for sensorless drives.

Chapter 2

METHODS OF SENSORLESS OPERATION

There are essentially two methods of controlling a sensorless BLDC motor. Each of these methods have several variations that are based on similar principles. One method that is used on sinusoidal BLDC motors involves the use of an estimator to determine the rotor position. Estimator techniques use the phase voltages and currents to determine the rotor position. This method is discussed in section 2.1 and is included only for completeness. The other method which can only be applied to trapezoidal BLDC motors involves detecting when the rotor passes a known position. The most popular variation of this method is discussed in section 2.2.1. Section 2.2.2 describes another variation, which is the focus of this thesis. The disadvantages of this second variation are discussed in detail in section 2.3. This will provide the motivation for the proposed modifications which will be detailed in chapter 3.

2.1 ESTIMATOR BASED POSITION DETECTION

There are several estimator based techniques [2] for controlling brushless DC machines, however most of these techniques are only applicable to motors with

sinusoidally distributed windings. The sinusoidal flux and induced voltage eliminate many of the discontinuities found in trapezoidal machines and make this type of motor well suited for coordinate transformations. Generally currents, voltages and sometimes fluxes are transformed into two-phase quantities. Usually the two-phase quantities are referred to the rotor frame of reference which decreases their time rate of change. The transformation to the rotor frame of reference is done with an estimate of the rotor position which generally contains some error. An observer is then used to drive this error to zero.

Stator currents cannot be used to calculate rotor position unless they are in some way effected by the back emf. Therefore the motor must be driven to some minimum speed before any estimation based technique may be used to control the motor.

Estimator techniques for controlling BLDC motors may require sophisticated control hardware including either a microcontroller or digital signal processor.

Estimation based control offers the advantage of fast torque/speed control since the phase currents and voltages are monitored at a very fast rate which is independent of the rotor speed. Unfortunately there has been little or no work done on applying advanced control techniques such as estimation and adaptation to trapezoidal BLDC motors.

2.2 DISCRETE POSITION DETECTION

Trapezoidal BLDC motors operate with only two phases conducting at a time.

This leaves the open phase available for detecting the rotor position. The rotor position is

detected only a fixed number of times per revolution, so it is desirable to have the detection occur long enough before the next commutation so that the delays associated with commutation can be accounted for. But if the detection occurs to soon before the next commutation a dynamic load may change the rotor speed and cause the commutation to occur at the incorrect time.

Section 2.2.1 describes a method of rotor position detection for trapezoidal BLDC motors that is called zero crossing detection. There are several implementations of zero crossing detection as described in [1] and [3], however the basic principles are the same. General Electric (GE) has used this method in many of their products that contain compressors. Another implementation of zero crossing detection, as proposed by Iizuka et. al. in the work of [3], has been used in air conditioner units since the early 1980's.

Section 2.2.2 describes another method for position detection that was proposed by Ogasawara and Akagi [4] in 1991. This method is the basis for the rest of this thesis. As will be seen in chapter 3 there are several modifications which can be made to make Ogasawara's method more effective.

2.2.1 ZERO CROSSING DETECTION METHOD

Zero crossing detection is a widely used sensorless operating method for trapezoidal BLDC motors. This method relies on the nearly trapezoidal shape of the line-to-neutral induced voltages. Figure 2.1 shows the shapes of the line-to-neutral induced voltages and the switching pattern that corresponds to proper commutation.

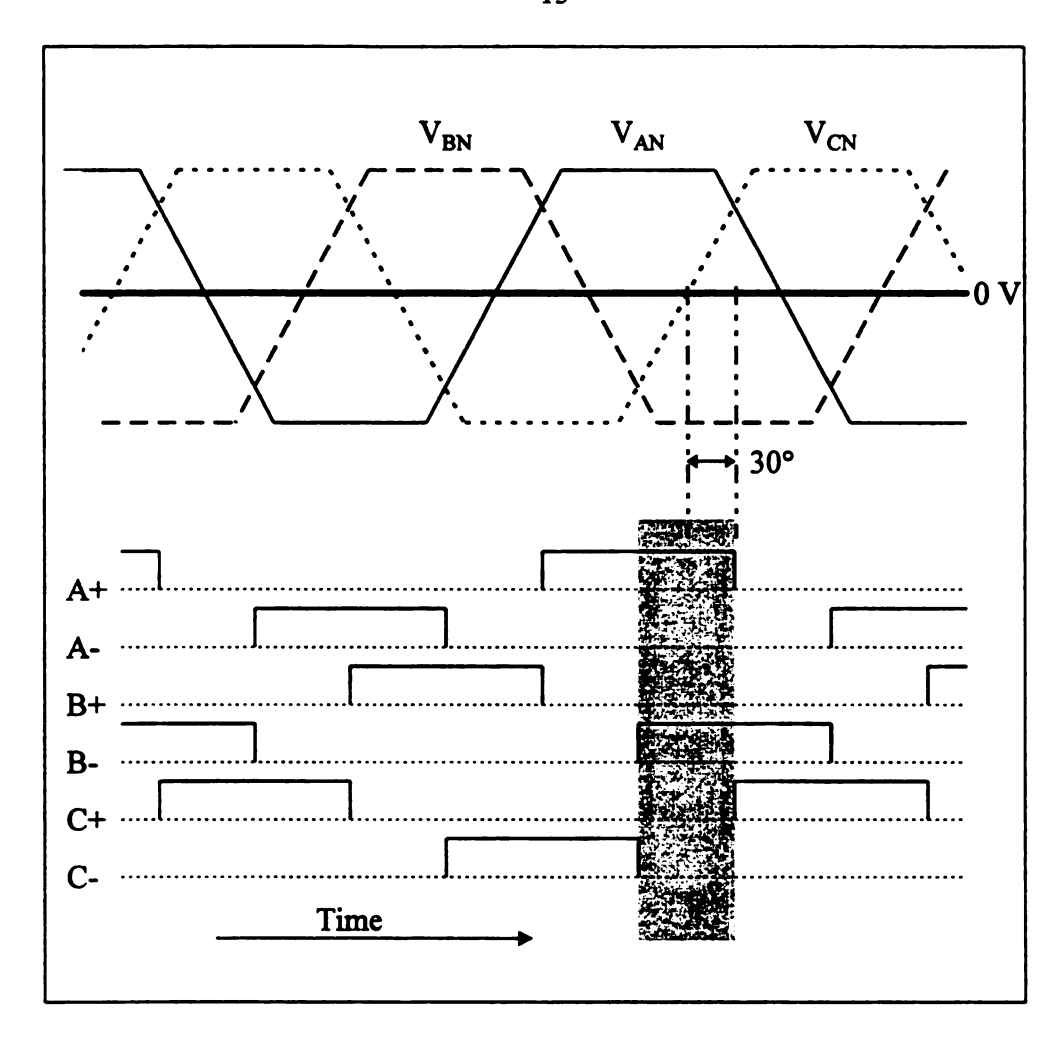


Figure 2.1 - Line-to-Neutral Back EMF and Corresponding Switching Events

The Shaded Area of Figure 2.1 indicates the period in which phase A is connected to the negative DC rail, phase B is connected to the positive DC rail and phase C is open circuited (only transistors A+ and B- are conducting). Notice that the next commutation occurs thirty electrical degrees after the line-to-neutral voltage V_{CN} crosses the zero voltage level. So if the line-to-neutral induced voltages can be measured, then the proper commutation time can be determined.

Since phase C is open circuited, there is no voltage drop across the resistance or inductance of that phase. This means that the induced voltage in phase C is present at the motor terminal. If the neutral voltage is known then V_{CN} can be easily determined.

The neutral voltage can be determined easily from the equivalent circuit as one half of the sum of the terminal voltages of the conducting phases minus one half of the sum of the induced voltages of the conducting phases. From Figure 2.1 it can be seen that in the area of interest the sum of the induced voltages in the conducting phases (phase A and B in this example) is zero. Therefore the neutral voltage is one half of the sum of the terminal voltages of the conducting phases. This is the method that GE in [1] uses to determine the neutral voltage. In the work of [3], the neutral voltage is determined by examining the neutral of a wye connected resistive load that is fed by the voltage at the motor terminals.

After the neutral voltage is determined, a comparator can be used to indicate the instant that the induced voltage in phase C crosses zero. A motor operating with zero crossing detection can be controlled very similarly to a motor with Hall-effect sensors except that the delay of thirty degrees from the point where the detection occurs to the point when the next commutation occurs must be compensated for.

Zero crossing detection can work at low speeds since the induced voltage only needs to be detected and not actually measured. The starting procedure in [3] requires that the motor reach a minimum speed of 200 rpm before the closed loop control is initiated. Unlike the method proposed in the following section, zero crossing detection does not require the DC rail voltage to be chopped.

2.2.2 OGASAWARA AND AKAGI'S METHOD

In 1991 Ogasawara and Akagi [4] proposed an alternate method of rotor position detection. This method is not based on terminal voltage measurements, but on the conducting state of a free-wheeling diode in the open phase of the inverter. Consider the equivalent circuit of the motor and inverter when transistors A+ and B- are conducting as shown in Figure 2.2. In Figure 2.2 the solid lines of the inverter represent the sections that are conducting current. The equivalent circuit of the motor including the winding resistance, inductance and induced voltages are also shown in Figure 2.2. The winding resistance and inductance are usually the same for each phase so $R_A = R_B = R_C = R$ and $L_A = L_B = L_C = L$. The induced voltages V_{AN} , V_{BN} and V_{CN} can be seen in Figure 2.1.

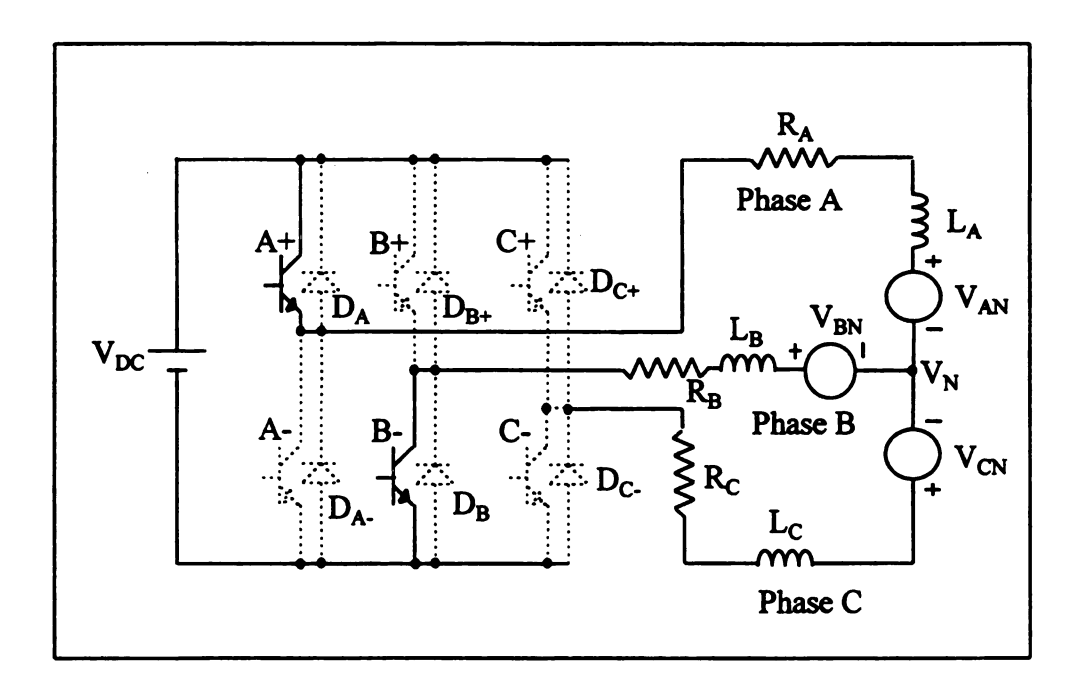


Figure 2.2 - Inverter and Motor with A+ and B- Conducting

Since no current is present in phase C, only the neutral voltage and the terminal voltage are needed to determine V_{CN} . The neutral voltage referenced to the negative DC rail can be expressed as shown below:

$$V_{N} = V_{DC} - V_{CE} - R \cdot i - L \frac{di}{dt} - V_{AN}$$

$$= V_{CE} + R \cdot i + L \frac{di}{dt} - V_{BN}$$

$$\Rightarrow$$

$$V_{N} = \frac{1}{2} (V_{DC} - V_{AN} - V_{BN})$$

where V_{CE} is the voltage drop across the transistor during conduction and i is the current through phases A and B. Figure 2.1 shows that when transistors A+ and B- are conducting, the induced voltages V_{AN} and V_{BN} are equal in magnitude and opposite in sign. This implies that the V_{N} is simply one half of the DC rail voltage.

Now, if the rail voltage is chopped by turning off transistor B- for a short time, the inductance of the motor will cause current to flow through the free-wheeling diode D_{B+} until the current stops. Figure 2.3 shows the equivalent circuit when transistor B- is not conducting and current flows through diode D_{B+} . Again the solid lines on the inverter represent the parts that conduct current.

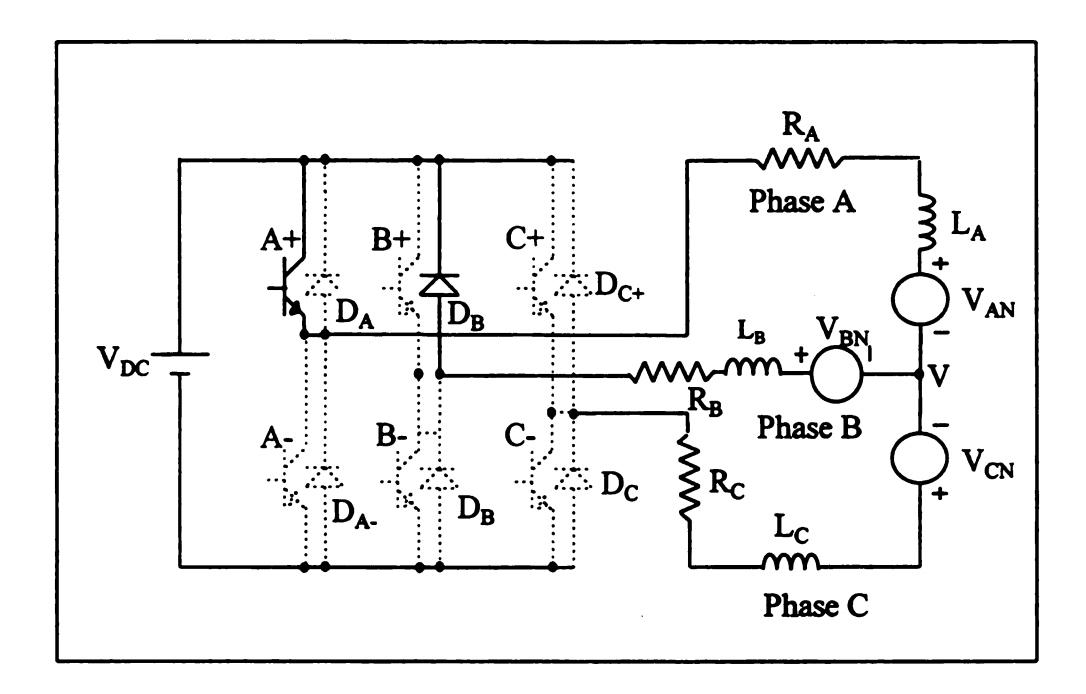


Figure 2.3 - Inverter and Motor with D_{B+} and A+ Conducting

The neutral voltage referenced to the negative DC rail can now be derived as shown below:

$$\begin{split} V_N &= V_{DC} - V_{CE} - R \cdot i - L \frac{di}{dt} - V_{AN} \\ &= V_{DC} + V_D + R \cdot i + L \frac{di}{dt} - V_{BN} \\ \Rightarrow \\ V_N &= V_{DC} + \frac{1}{2} (V_D - V_{CE} - V_{AN} - V_{BN}) \end{split}$$

where V_D is the forward biased voltage drop across a free-wheeling diode. As mentioned above, the induced voltages in phase A and B are approximately equal in

magnitude and opposite in sign in the period of interest (see the shaded portion of Figure 2.1). Therefore during the short period of time in which D_{B+} conducts the neutral voltage can be expressed as shown below:

$$V_N = V_{DC} + \frac{1}{2}(V_D - V_{CE})$$

Notice that the voltage at the motor terminal of phase C is $V_N + V_{CN}$ referenced to the negative DC rail. If the terminal voltage becomes greater than $V_{DC} + V_D$, then the freewheeling diode D_{C+} will start to conduct. The derivation below shows the line-to-neutral induced voltage that causes the diode D_{C+} to conduct.

$$V_{CN} + V_N \ge V_D + V_{DC}$$

$$\Rightarrow V_{CN} \ge -V_N + V_{DC} + V_D$$

$$\Rightarrow V_{CN} \ge -V_{DC} + V_{DC} - \frac{1}{2}V_D + V_D + \frac{1}{2}V_{CE}$$

$$\Rightarrow V_{CN} \ge \frac{1}{2}(V_D + V_{CE})$$

Typically V_D and V_{CE} are between one half and one volt. So as V_{CN} goes slightly positive, the free wheeling diode D_{C+} will start to conduct. Similarly to zero crossing detection as described in section 2.2.1 conduction occurs for the first time approximately thirty electrical degrees before the next commutation. It is important to note that the zero

crossing of the back emf causes the free wheeling diode to conduct but that the zero crossing itself is not detected.

Notice that if the analysis above is performed for the case when transistors A+ and C- are conducting, then the transistor A+ will need to be chopped. This means that after 360 electrical degrees each transistor will go through a state where it is conducting for sixty degrees and chopped for sixty degrees. Figure 2.4 shows the induced line-to-neutral voltages and corresponding switching states. The shaded area of the switching states indicate that the transistor is being chopped.

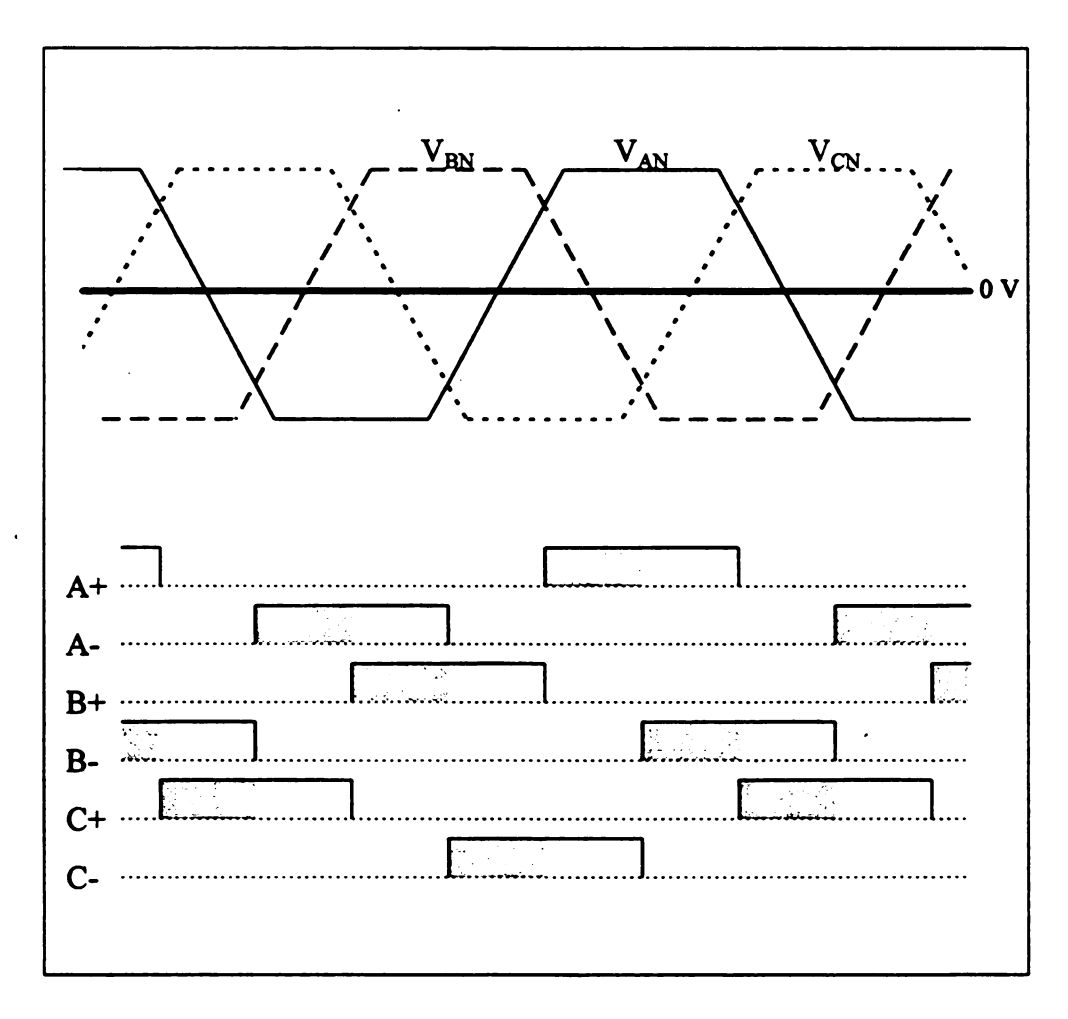


Figure 2.4 - Line-to-Neutral Back EMF and Switching Events Including Chopping

To detect the conducting state of the freewheeling diodes another diode and resistor can be placed in anti-parallel with each free-wheeling diode. The voltage drop across the extra diode can be measured by a comparator as described in [4]. Figure 2.5 shows the structure of the detection circuit proposed by [4]. Note that one of these circuits must be connected to each phase of the inverter.

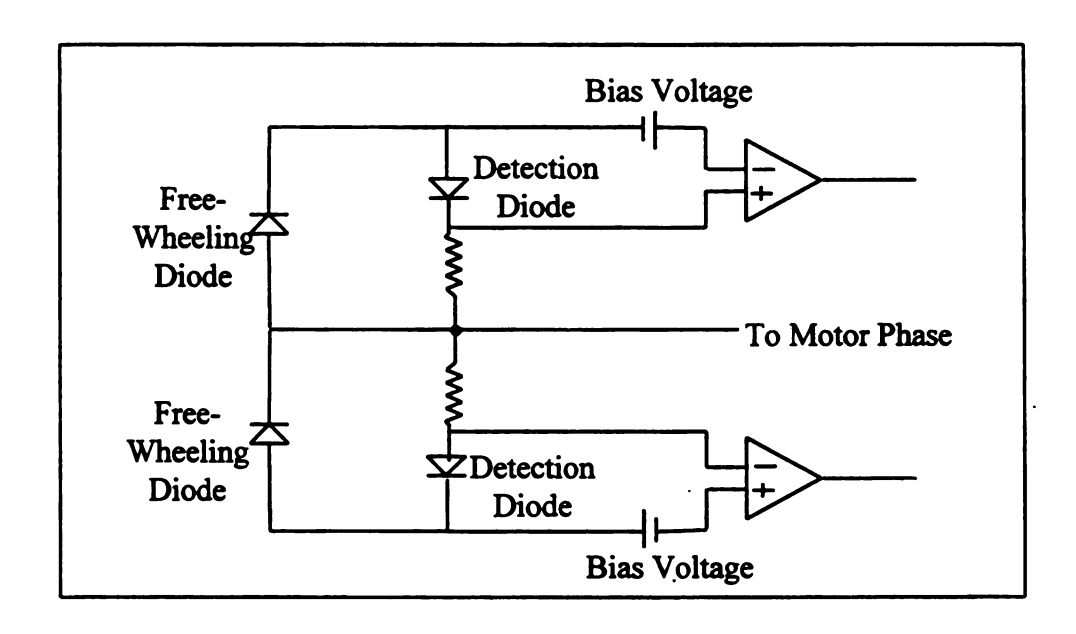


Figure 2.5 - Detection Circuit Using Floating DC Supplies

In the work of [4] the control of the motor is done very simply using a multiplexer to select which comparator output to use and a digital phase shifter to implement the thirty electrical degrees of delay that is needed for the next commutation signal.

The method proposed by Ogasawara and Akagi works at very low speeds (45 rpm in [4]) since the diode conduction occurs whenever the induced voltage is greater than the

average of the forward voltage drop across the freewheeling diode and the conducting voltage drop across the power transistor (typically one half to one volt).

Since the minimum detection speed is so small, a very simple starting procedure can be employed. As with any sensorless motor operating scheme the first time any two phases are energized the rotor will move either forward or backward. If the phases are energized long enough, the rotor will come to rest at a position where there is zero total torque on the rotor. It should be noted that for a two pole machine there are two equilibrium points for the rotor but only one stable equilibrium point. Therefore the rotor will come to rest in only one position (assuming that friction is insignificant). Figure 2.6 shows a cross-section of the motor when two predetermined phases are energized and the rotor has reached the stable equilibrium point. The circles in the stator indicate the direction of current flow. The arrows in the air gap indicate the direction of the torque caused by the Lorentz force (B×i).

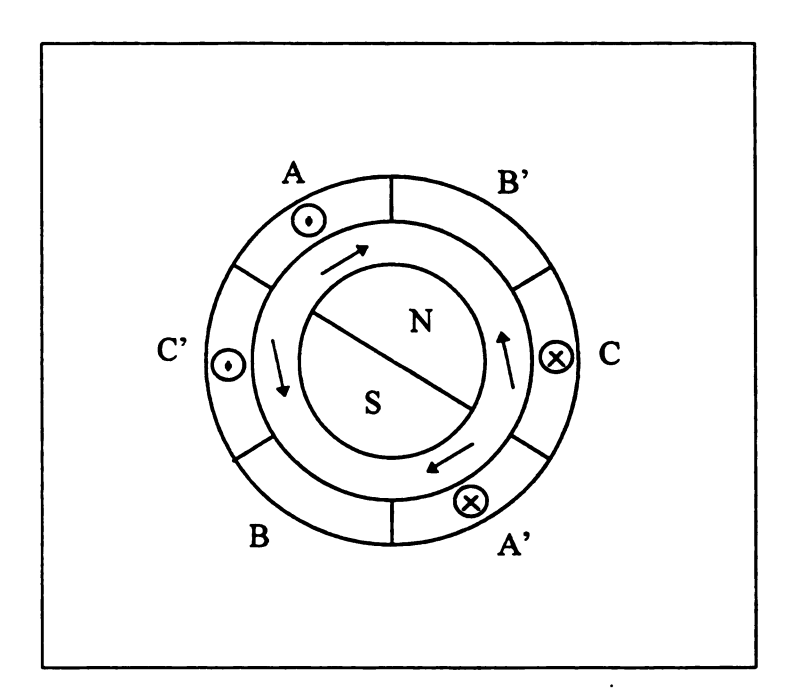


Figure 2.6 - Motor Cross Section During Initialization of Starting Procedure

If the next commutation then advances the switching sequence by 120 electrical degrees (two steps) the rotor will accelerate at a constant rate for sixty degrees (assuming constant load). The acceleration is constant because the current is constant and the flux from the magnet pole will be constant (therefore the torque will be constant) for the next sixty degrees. The rate of acceleration is proportional to the current through the conducting phases. Figure 2.7 shows the motor cross-section after this commutation.

Since the minimum detection speed is so low, the next commutation can be performed automatically by the diode conduction detection circuit and the control hardware. So the starting scheme consists of an initialization and only one additional open loop commutation.

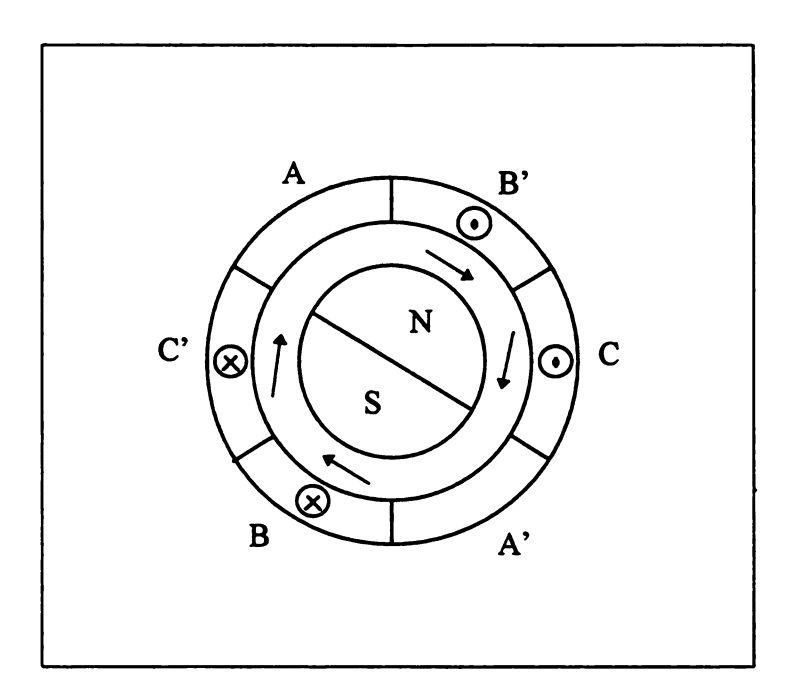


Figure 2.7 - Motor Cross Section During Second Phase of Starting Procedure

This discrete rotor position detection method allows very low operating speeds and a simple, short starting procedure. However, there are several disadvantages to this method which make it less attractive than zero crossing detection. If these disadvantages can be overcome, the simple starting procedure and low operating speeds will make this method superior to zero crossing detection.

2.3 DISADVANTAGES OF OGASAWARA AND AKAGI'S METHOD

The disadvantages of the discrete rotor position detection method of section 2.2.2 can be grouped into three categories. The first category is disadvantages associated with

the implementation of the detection circuit. The detection circuit described in section 2.2.2 requires six isolated voltage supplies, which are difficult to implement in a manor which is both inexpensive and durable.

The second category is disadvantages associated with the operating range of the motor. Proper explanation of this problem is the subject of section 2.3.1. The third category is disadvantages associated with dynamic performance, and is discussed in section 2.3.2.

2.3.1 DIFFICULTY IN MAXIMIZING MOTOR OPERATING SPEED RANGE

The sensorless operating scheme described in section 2.2.2 detects the rotor position only the instant that the inverter chops. Therefore the time at which conduction of the free-wheeling diode is detected may be as much as one chopping period after the zero crossing of the back emf occurred. This means that when the rotor speed becomes comparable to the chopping frequency the time when the freewheeling diode conducts may be become significantly different from the time when the induced voltage crosses zero as shown in Figure 2.8.

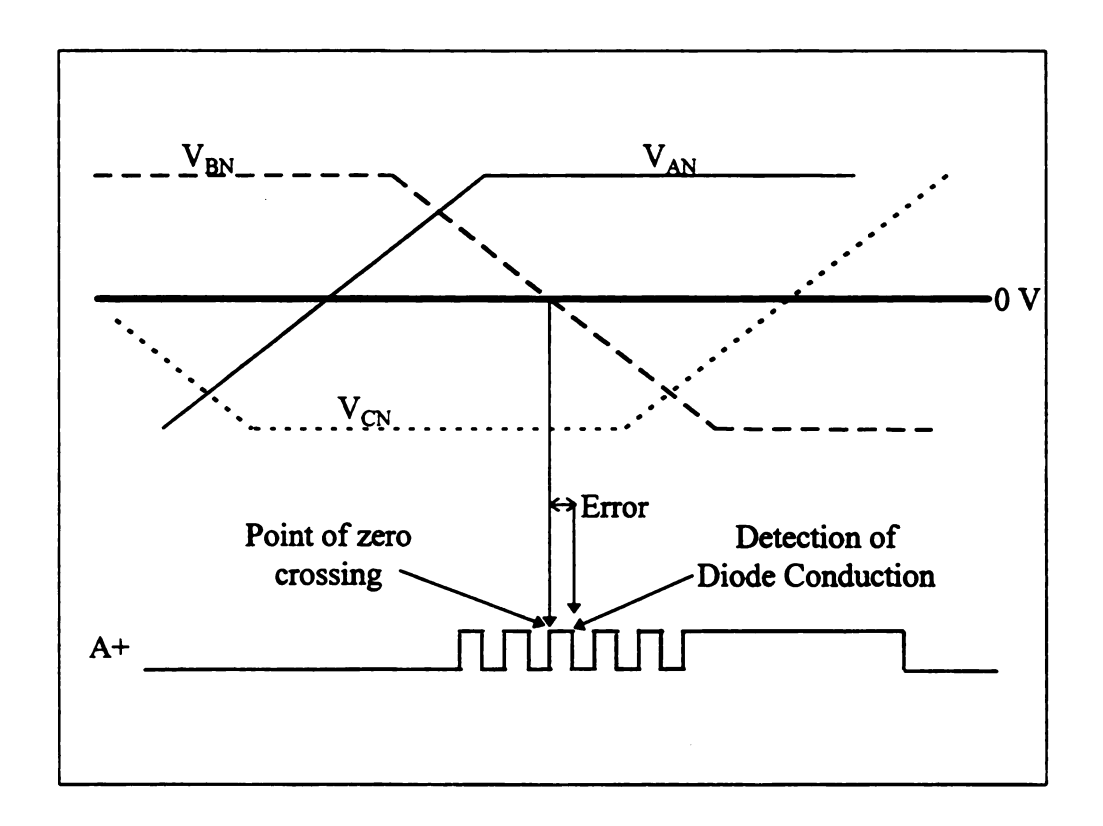


Figure 2.8 - Detection Error at High Speeds

If high rotor speeds are desired, the chopping frequency must be comparably high.

In [4] the chopping is performed at a fixed frequency regardless of rotor speed. Chopping at high frequencies causes an increase in switching losses at all rotor speeds. A simple way to lessen the degree of this problem is described in chapter 3.

In addition to the error that occurs at high speeds, an additional error occurs at low speeds as well. This error becomes significant when the induced voltage becomes comparable with the minimum voltage needed to cause the free wheeling diode to conduct. For example, Figure 2.9 shows a motor that has a peak-to-peak induced voltage

of K_v [Volts/rpm]. If the average voltage drop of the inverter free wheeling diodes and conducting transistors is K_c [Volts], the induced voltage must become greater than or equal to K_c for the free wheeling diode to conduct. Figure 2.9 shows the case when the rotor speed is low enough that the induced voltage is comparable to the voltage that is needed for the free wheeling diode to conduct.

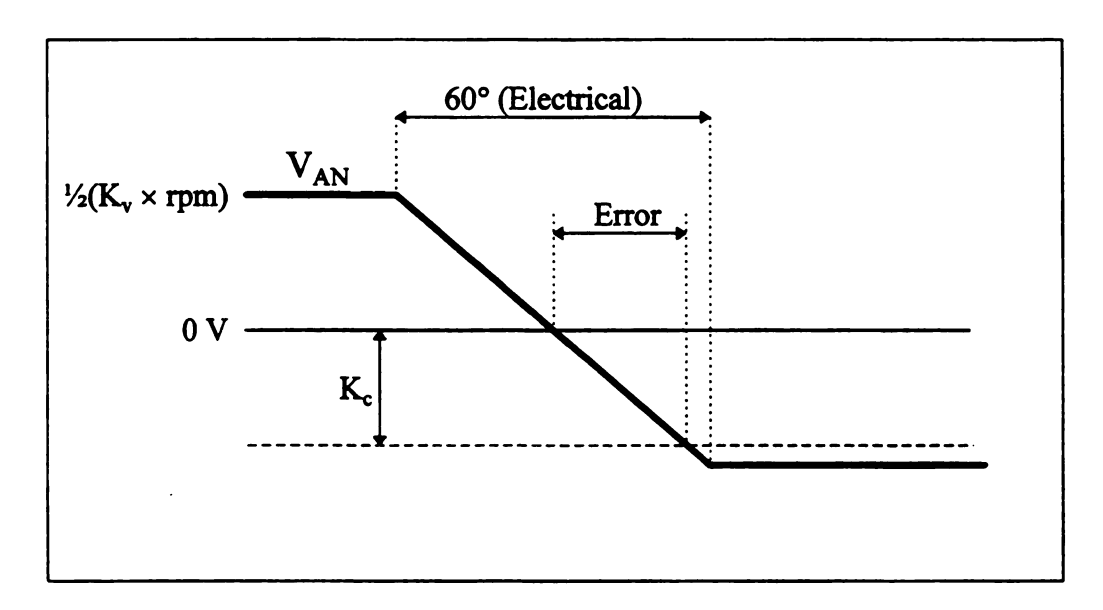


Figure 2.9 - Detection Error at Low Speeds

For the machine to operate at its minimum possible speed, the digital phase shifter described in [4] should account for this error. The phase shifter in [4] does attempt to account for this error, but it does so by simply commanding the commutation to occur as soon as the conduction is sensed whenever the rotor speed is below some predetermined value. This is clearly not an optimal solution if the motor is intended to operate at low speeds for any significant amount of time.

2.3.2 PROBLEMS WITH DYNAMIC PERFORMANCE

The DC rail voltage must be chopped so that the diode will conduct. Aside from increased switching losses, this results in other dynamic performance losses. Since there is always chopping, the maximum DC voltage can never be applied to the motor. This results in a lower maximum speed and a lower maximum acceleration for any load.

Similarly to zero crossing detection, the rotor position is detected thirty electrical degrees before the next commutation. The delay is large enough that a very dynamic load could change the rotor speed enough to cause a misprediction of the commutation time. The digital phase shifter with programmable delay used in [4] was made to account for linear accelerations, but it will always mispredict the commutation instant when the acceleration begins and when the acceleration ends. If the magnitude of this misprediction is large enough, the motor will not run smoothly and the phase current may become exceptionally large. If the load disturbance causes the rotor to slow down, the next commutation may occur so early that the motor will not be able to deliver enough torque to complete the rotation and the motor will stall.

With the exception of the problems discussed in the previous paragraph, all of the disadvantages to this method of sensorless operation can be overcome or lessened by the modifications proposed in chapter 3. These modifications may also lead to the eventual elimination of all of the disadvantages to this method (including those mentioned in the previous paragraph) as discussed in chapter 6.

Chapter 3

MODIFICATIONS TO OGASAWARA AND AKAGI'S METHOD

In Ogasawara and Akagi's method, the conducting state of the a free-wheeling diode in the inverter is used to determine the rotor position. As mentioned before this scheme allows the motor to operate at very low speeds. In fact the operating speed is so low that the motor can be started by moving the rotor to some initial position and then providing only one additional open loop commutation. However this method has several disadvantages as described in section 2.3.

Section 3.1 is dedicated to proposed solutions to many of the problems presented previously. In this section a new detection circuit is proposed that eliminates the need for six isolated voltage supplies (see Figure 2.5). In addition to this the digital phase shifter is replaced by a microcontroller which can be used eliminate the errors that occur at high and low rotor speeds as described in section 2.3. The microcontroller can also chop in a more selective manor so that some of the dynamic problems mentioned before can also be lessened. The addition of the microcontroller and its increased abilities make it possible to go even further to enhance the dynamic performance of the motor. This will be discussed in chapter 6, and has yet to be implemented.

3.1 PROPOSED IMPROVEMENTS

Since the conduction of current in the free-wheeling diode corresponds to current in the "open" phase of the inverter, the phase current can be sensed instead of the voltage drop across the diode. Phase current detection can be done by adding a very small resistor in each of the motor phases. This is already done many applications to implement overcurrent detection. Or current can be sensed using current transducers. Inverters for automotive and other applications may already contain three current transducers so there should be little or no cost for this implementation.

The use of current transducers provides isolation between the phases and the rest of the detection logic and makes it possible to implement current detection without the use of isolated voltage supplies. Figure 3.1 shows the proposed current detection circuit. Notice that the bias voltages for the comparators can be implemented with batteries or more conveniently with operational amplifiers since they reference a common ground. One of these circuits should be used for each motor phase. Ideally the bias voltage supplies for all six comparators could be implemented with only two operational amplifiers. The value of the bias voltage depends on the current transducer and comparator.

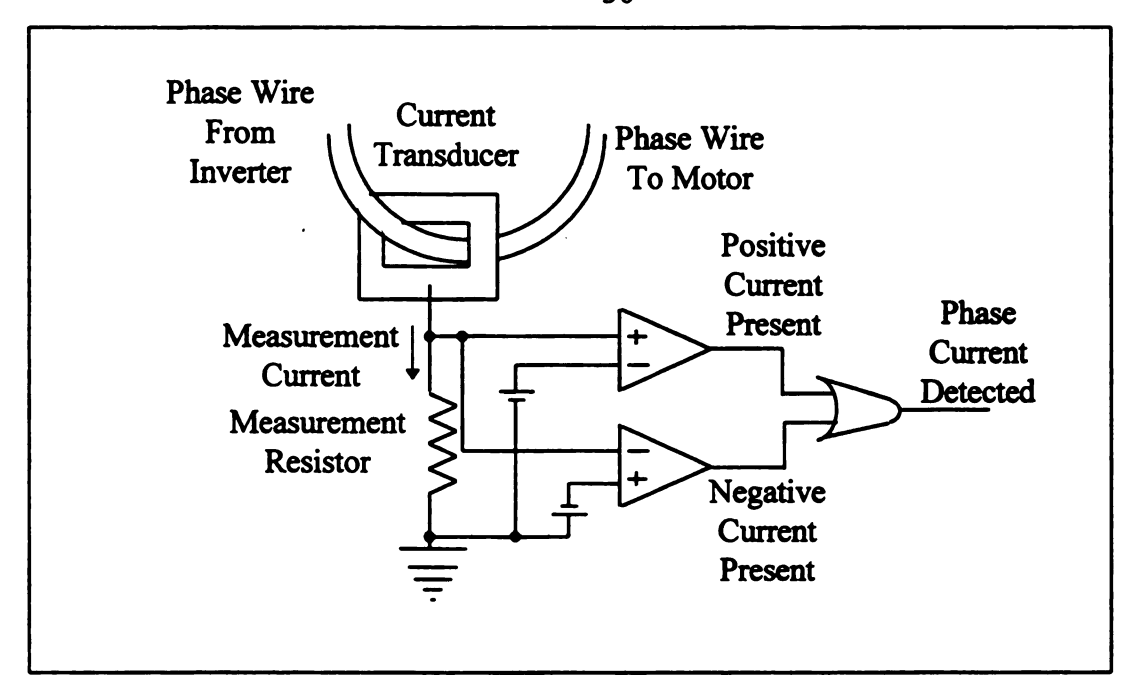


Figure 3.1 - Detection Circuit Implemented with Current Transducers

When the motor is running with the proper chopping scheme the input and output of the detection circuit will look like the waveforms in Figure 3.2.

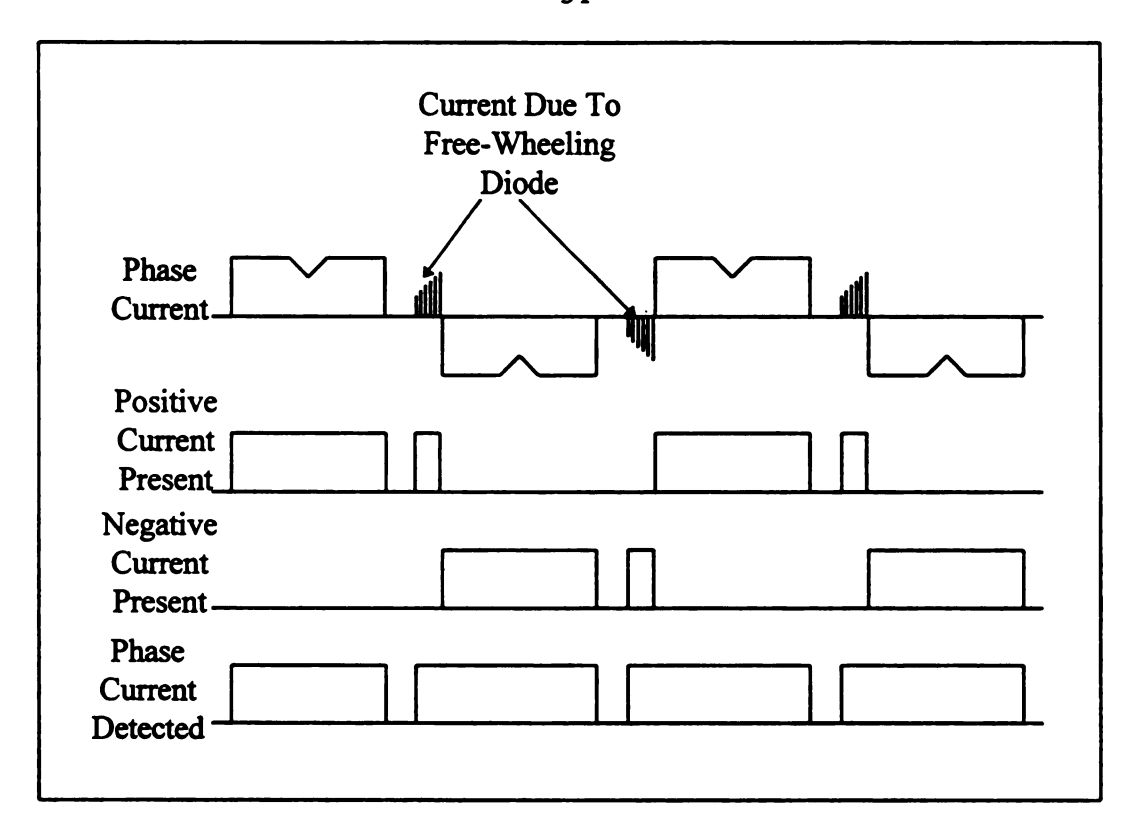


Figure 3.2 - Waveforms of the Current Detection Circuit

Of course the output of the detection circuit should only be monitored at the proper time. Therefore there must be additional logic to gate the proper circuit output to the controller.

To eliminate the errors that occur at high rotor speeds (see section 2.3.1), the microcontroller can adjust the chopping frequency as the rotor speed changes. This means that the chopping frequency does not need to be unnecessarily high at low rotor speeds. This will result in lower switching losses and still allow high rotor speeds. The chopping frequency can be adjusted continuously as rotor speed changes, or one of only two or three predetermined chopping frequencies can be selected as the rotor speed

reaches calibrated thresholds. Unfortunately the maximum rotor speed will still be limited by the maximum chopping frequency of the inverter.

The error in detecting the zero crossing at low rotor speeds (see section 2.3.1 and Figure 2.9) can also be corrected by the microcontroller. The value of the error shown in Figure 2.9 can be calculated using the following formula:

$$Error = 10 \frac{K_C}{K_W} \left(\frac{2}{P}\right) \frac{1}{rpm^2} \quad [seconds]$$
 (1)

where P is the number of poles the machine contains, and K_c and K_v are the minimum induced voltage for detection and the motor voltage constant respectively (see Figure 2.9). Of course an alternate expression for this equation can be derived for more convenient calculations inside the microcontroller.

Since chopping is required to detect the rotor position, the motor cannot achieve maximum speed or maximum acceleration. This effect can be lessened if the chopping is stopped just after current is detected in the open phase until the next commutation begins. This will result in approximately 50% less chopping when the motor is commanded to operate at its maximum voltage. Although this does not eliminate the problem it is certainly a step in the right direction. This irregular chopping scheme may result in torque oscillations. The experimental results (see chapter 5) discuss this potential problem.

3.2 PROPOSED SENSORLESS OPERATING SCHEME

The system proposed for operating the motor without rotor position sensors is represented in Figure 3.3.

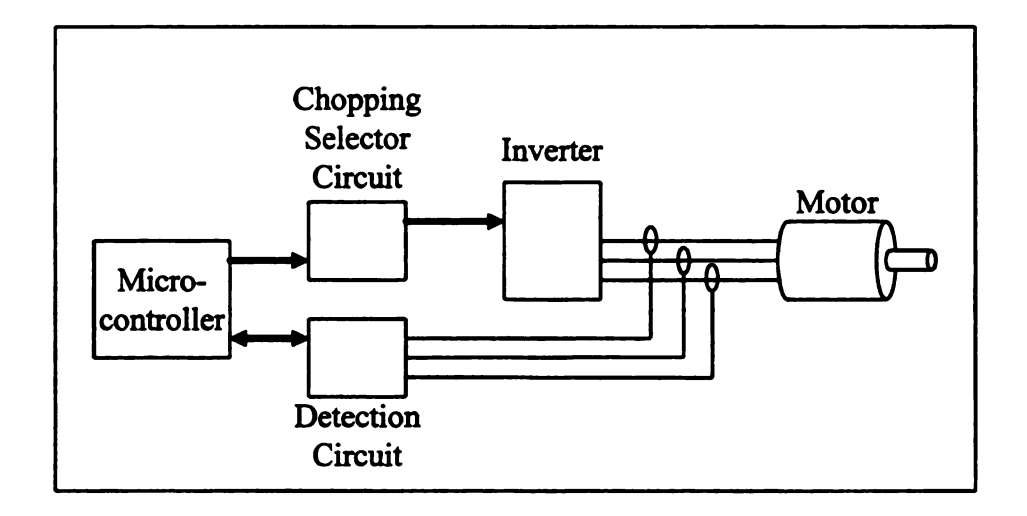


Figure 3.3 - Proposed System for Sensorless Operation

The detection circuit is similar to that of Figure 3.1 except that three of the circuits will be required (one for each phase) and extra logic is needed so that the microcontroller can select which circuit output to read at the proper time. The chopping selector circuit determines which transistor to chop. This function could be performed by the microcontroller, but since the circuit is almost entirely combinational logic, it can be easily implemented externally.

The microcontroller performs all of the calculations needed to determine the commutation time. It must first perform the simple starting procedure, then determine

which phase current to monitor. After the current is detected in the open phase, the microcontroller can use any of a variety of methods to predict the time for the next commutation. The simplest prediction scheme is one in which the microcontroller determines the time at which the current detection occurs ("B" in Figure 3.4) and compares that time to the time of the last commutation ("A" in Figure 3.4). The change in time ("ΔT" in Figure 3.4) will then be added to the detection time to determine the time for the next commutation as shown in Figure 3.4.

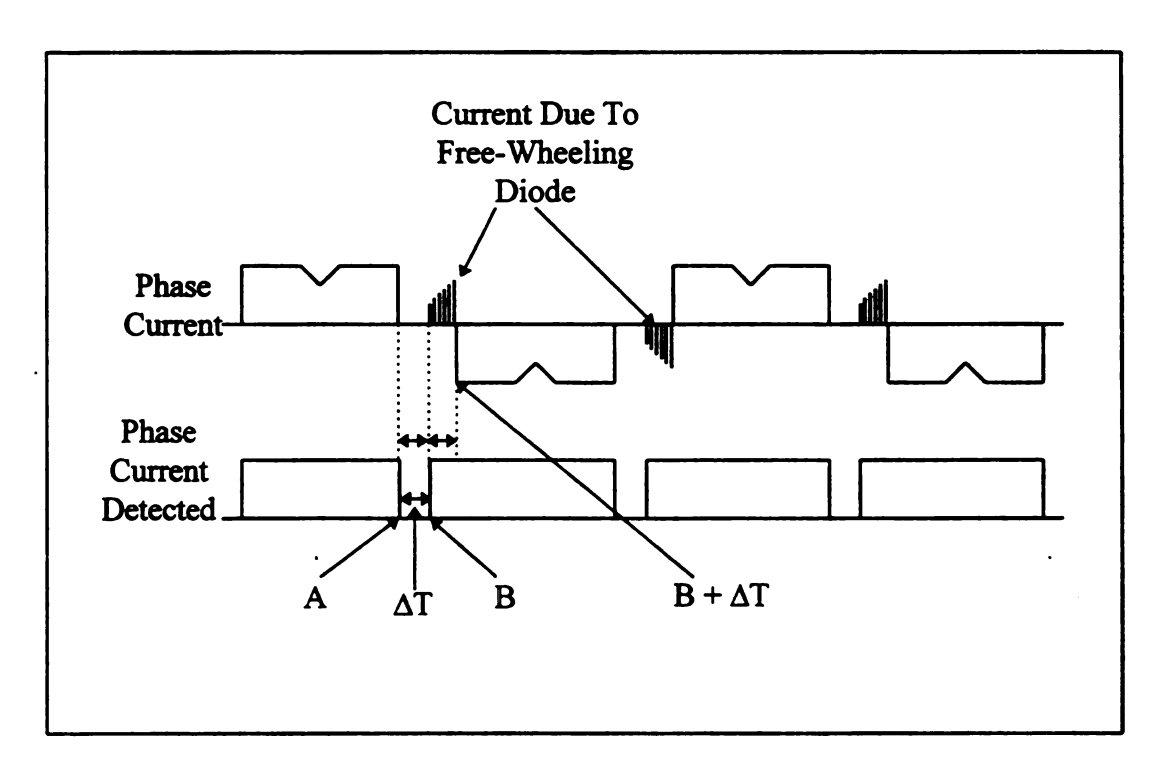


Figure 3.4 - Simple Method of Commutation Time Prediction

Alternately, the microcontroller can compare the time at which current is detected in the open phase ("B" in Figure 3.5) with the last time current was detected in the last open phase ("A" in Figure 3.5) and add one half of the difference (" Δ T" in Figure 3.5) to the most recent time that current was detected as shown in Figure 3.5.

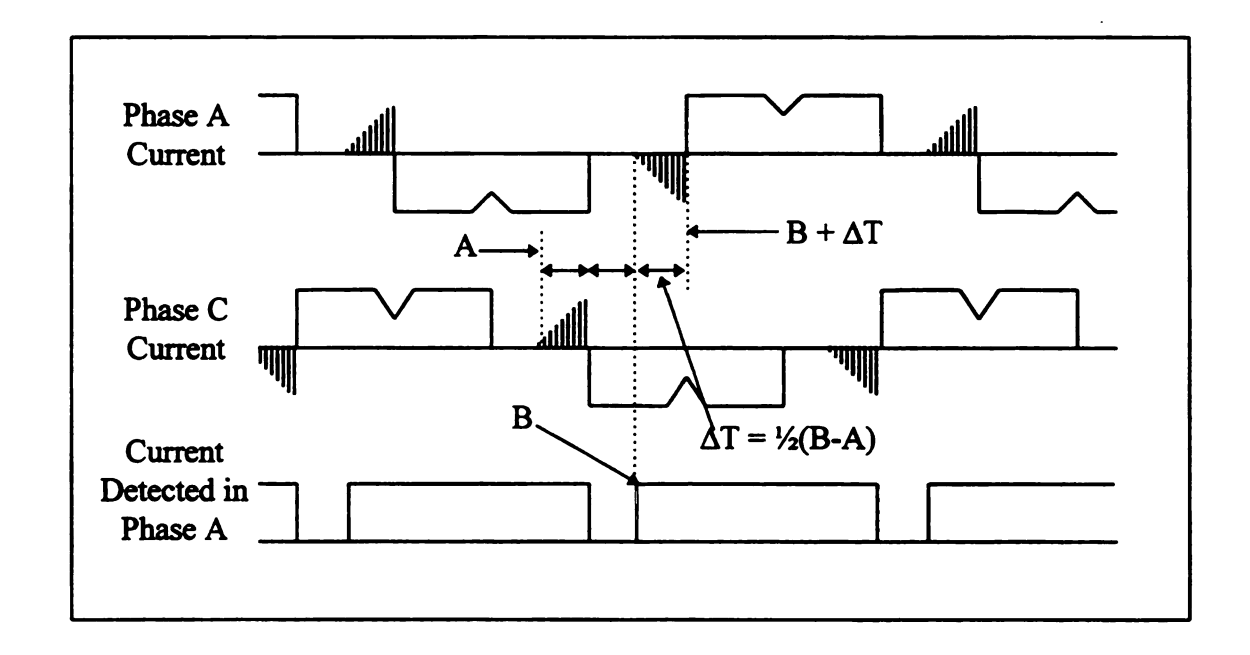


Figure 3.5 - Preferred Method of Determining Commutation Time

In addition to either of these prediction schemes, the microcontroller must also compensate for the low speed errors associated with (1). At high speeds, the microcontroller must also increase the chopping frequency. When the inverter is chopping at maximum duty cycle, the microcontroller should also signal the chopping

selector circuit to stop chopping after current is detected in the open phase as described before. The implementation is this system is described in Chapter 4.

Chapter 4

EXPERIMENTAL SETUP

An experiment was performed to test Ogasawara and Akagi's method with the proposed improvements. This chapter describes the hardware and software used in the experiment. This chapter is organized into sections that correspond to the components of the proposed system as shown in Figure 3.3.

4.1 CHOPPING SELECTOR CIRCUIT

The chopping selector circuit of Figure 3.3 was implemented by the circuit shown in Figure 4.1. The circuit represented in Figure 4.1 is slightly redundant, and contains some extra logic to protect the inverter.

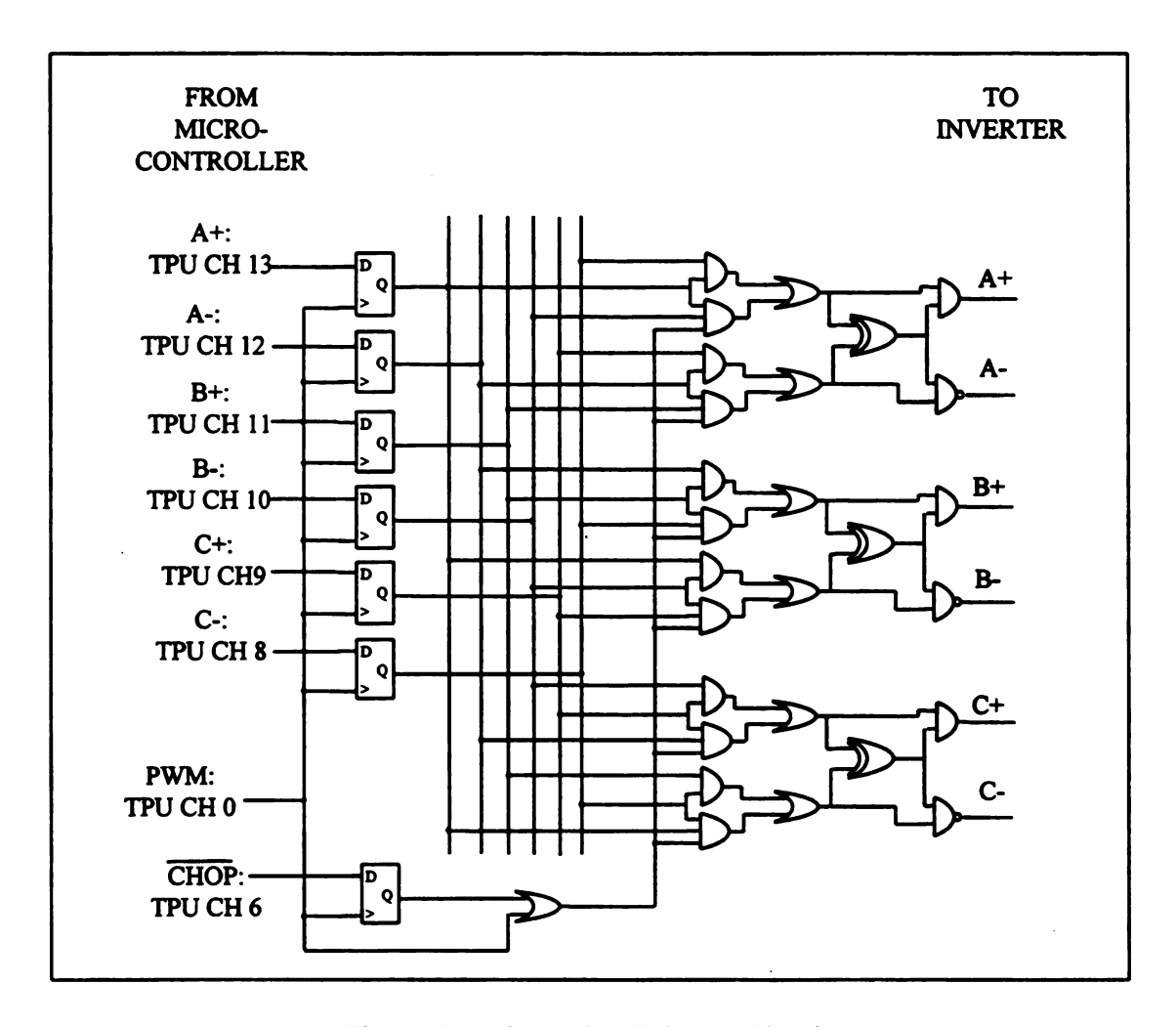


Figure 4.1 - Chopping Selector Circuit

The microcontroller simply indicates which phases should be energized, provides the chopping waveform, and indicates whether or not chopping is to be allowed. The selector circuit applies the chopping waveform to the appropriate phase. The D-type flip-flops are used to ensure that any change in inverter state will be synchronized with a change in the PWM signal. This is done to ensure that a phase cannot be turned "on" and "off" again in an extremely short amount of time for the protection of the inverter.

The exclusive-OR gates are used for protection against shoot-through. Shoot-through is caused when any two transistors in a given phase (i.e. A+ and A-) are conducting at the same time. This causes a large current flow through the transistors and can destroy the inverter.

As indicated by the use of both AND and NAND gates in the final stage of the circuit, the inverter allows the transistors that are connected to the positive rail (A+, B+, and C+) to conduct with high inputs. However the transistors connected to the negative rail (A-, B-, C-) are active low.

To disable chopping the microcontroller simply sets the value of CHOP high.

This is only done when the PWM is at its maximum duty cycle and after the current has been detected in the open phase.

4.2 **DETECTION CIRCUIT**

The detection circuit from Figure 3.3 was implemented using a circuit similar to that of Figure 3.1 but with some slight modifications. The experimental circuit for all of the phases is shown in Figure 4.2. The signal labels include the names of the microcontroller pins that either provide or receive the signal.

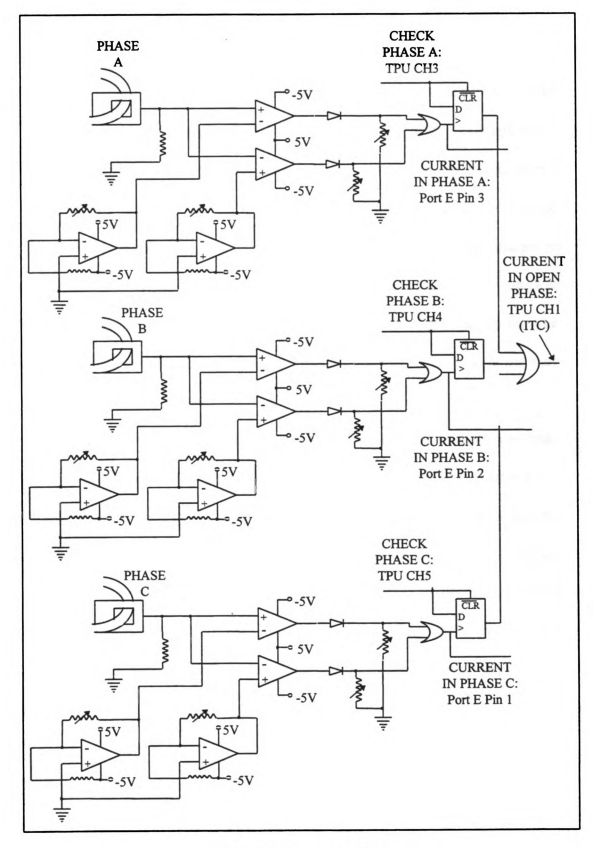


Figure 4.2 - Detection Circuit

The operational amplifies used for both comparators and bias voltage were number LF347 which contains four amplifiers per integrated circuit. Since these operational amplifiers were used with ±5 V rails, the diodes and resistors were needed so that a -5 V output would not be applied to the two-input OR gates. Although six operational amplifiers were used to generate the bias voltages for the comparators, fewer amplifiers (as few as two) may be used to generate the bias voltages for the three phases. Notice that the bias voltages are all positive. One would expect the bias voltages for the comparators that detect negative phase current (represented by a negative voltage across the measuring resistor) to be negative. However the internal bias of the op-amps and current transducers allow a small positive voltage to be used. The value of the bias voltages are less than 30 mV.

The structure of this circuit provides some insight into the control algorithm executed by the microcontroller. For example, if the microcontroller initiates a commutation in which phases C and B are conducting and phase A is open, then the signal labeled "CURRENT IN PHASE A" is monitored to ensure that the commutation is complete. After the current in phase A has decayed, the microcontroller sets the signal labeled "CHECK PHASE A". This allows the detection of any current in phase A to cause an interrupt to indicate that the induced voltage has just crossed zero.

4.3 INVERTER

The inverter used for the experiment was built in the Electric Machines Lab at Michigan State University. It consists of a power transistor module and a driver board. The transistor module (also known as a power module) used is an Intellimod PM30RFS060 manufactured by Powerex. This module contains the usual six IGBTs and free-wheeling diodes along with a seventh power transistor which can be used to short the DC rail. The forward voltage drop across a conducting free-wheeling diode (V_D) was measured to be 0.53 V. The saturation voltage drop across the power transistors (V_{CE}) was measured to be 0.99 V. The average of these two voltages is 0.76 V. This is the induced voltage need to cause a free-wheeling diode to conduct (K_c).

The power module also contains protection circuitry which may be activated when the transistors are too hot, conduct too much current, or are driven with improper voltages. The driver board provides isolation between the high voltage of the inverter and the TTL signals produced by the chopping selector circuit. It converts the six TTL signals into the six driving signals for the power module.

It should be mentioned that shoot-through protection is provided by two separate sources. First the power module has internal protection from shoot-through, however this protection is not intended to be used on a normal basis. In fact repeated activation of the shoot-through protection devices on the power module is considered to be misuse and can lead to damage. The second layer of shoot-through protection comes from the chopping

selector circuit of Figure 4.1. As mentioned before, the exclusive-OR gates prevent two transistors in the same phase from being accidentally turned on at the same time.

4.4 BRUSHLESS DC MOTOR

The motor used for the experiment was a four pole Bodine 3/8 HP trapezoidal brushless DC motor (type 34B6BEBL, model #3309). The motor is rated at 2.7 A and 2500 rpm. The rotor contains rare earth permanent magnets which produce an induced voltage of 42 mV/rpm peak-to-peak (K_v) in the stator. Since the free-wheeling diode will conduct when the magnitude of the induced voltage exceeds 0.76 V the theoretical minimum speed of the motor is 36.19 rpm.

The motor was originally intended to be operated using the three Hall-effect sensors attached to the back of the machine. These sensors were disconnected for the experiments.

4.5 MICROCONTROLLER

The microcontroller used for the experiment was a Motorola 68332. This is a 32-bit processor capable of operating at 16.67 MHz. The 68332 also contains a Time Processor Unit (TPU) which was used to facilitate the PWM and timing functions required to operate the motor. The processor contains two 8-bit parallel I/O ports (ports E and F) and the TPU has 16 channels which may be used as I/O or to implement any of the

"CURRENT IN OPEN PHASE" (Figure 4.2) use the parallel I/O port E. All of the microcontroller outputs are implemented using TPU channels as output pins since port E has only eight pins (port F was intentionally not used to leave room for future expansion).

The TPU's PWM function was used to facilitate chopping. This pre-programmed function generates a PWM signal of period and duty cycle specified by two registers.

This makes it possible to control the motor voltage by simply increasing or decreasing the value in the duty cycle register. The period register can be adjusted to increase or decrease the chopping frequency which will enable the motor to operate properly at high and low speeds as described earlier.

The TPU's Input Transition Counter (ITC) function was used to capture a timer value when the signal labeled "CURRENT IN OPEN PHASE" (Figure 4.2) transitions from low to high. This will also cause an interrupt. The interrupt service routine (ISR) for the ITC then calculates the time at which the next commutation should occur (actually just the difference between the current time and the next commutation time is calculated).

The first closed loop commutation time is calculated using the simple method shown in Figure 3.4. After the first closed loop commutation, the algorithm shown in Figure 3.5 is used. The slightly more complicated algorithm of Figure 3.5 is preferred since it is based on actual current detection and not a previous calculation. The more simplistic method of Figure 3.4 is used for the first closed loop commutation because it is easy to initialize since the time of the last open loop commutation can be used for initialization. Unfortunately an interrupt must be generated to capture the time of the last

open loop commutation. Therefore the first time the ITC ISR is executed the time of the last open loop commutation is captured. The second time the ITC ISR is executed the first closed loop commutation time is calculated using the method of Figure 3.4. During the third invocation (and during all subsequent invocations) of the ISR the commutation time is calculated using the method shown in Figure 3.5.

At low speeds, the commutation time (calculated by the method described above) must be corrected since the induced voltage is comparable to the voltage needed for the free-wheeling diode to conduct. Since all of the timing is done using a TPU timer, equation (1) must be modified to give the error in timer counts. Since the motor has four poles and the TPU timer is configured to run at 65.10 kHz, equation (1) can easily be modified as shown.

$$Error = \frac{4}{5} \frac{K_c}{K_v} (15.36 \cdot 10^{-6}) \Delta C^2$$
 [counts] (2)

where ΔC is the value of ΔT (from Figures 3.4 and 3.5) expressed in 15.36 μs increments.

Multiplying by the constant, 15.36×10^{-6} be can accomplished by shifting the binary value 16 places to the right, or taking only the high word of ΔC^2 if it is stored as a long word. This is not exact but produces less than 1% error. The values for K_c and K_v can be determined easily from the characteristics of the inverter and motor respectively. However the value of K_c determined from the inverter characteristics is only valid if the

detection circuit is able to detect infinitesimally small amounts of current. The actual back emf that must be obtained for the detection circuit to detect the rotor position on time must be determined through experiment (see section 5.1).

After the error is subtracted from the commutation time, the ITC ISR initializes another TPU function called an Output Compare (OC). The OC causes an interrupt at the calculated commutation time (from the ITC ISR). The OC interrupt service routine then initiates the commutation. The commutation is complete when a low voltage is present on the "CURRENT IN PHASE x" signal (x is the open phase) for a predetermined number of loops. The OC interrupt service routine then sets the proper "CHECK PHASE x" signal (x is the open phase) so that current in the open phase can cause another ITC interrupt. The OC ISR also adjusts the chopping frequency to allow high rotor speeds. Finally, the ITC interrupt is enabled, which causes the process to repeat indefinitely.

Figure 4.3 shows a flow chart for the control algorithm executed by the main program and ITC ISR. Figure 4.4 shows a flow chart for the OC ISR. Appendix A contains the actual assembly code which implements these functions. It should be noted that in the experiment, the motor spins in the opposite direction than that implied by Figures 2.1, 2.4, 2.6, 2.7, 2.8 and 3.5.

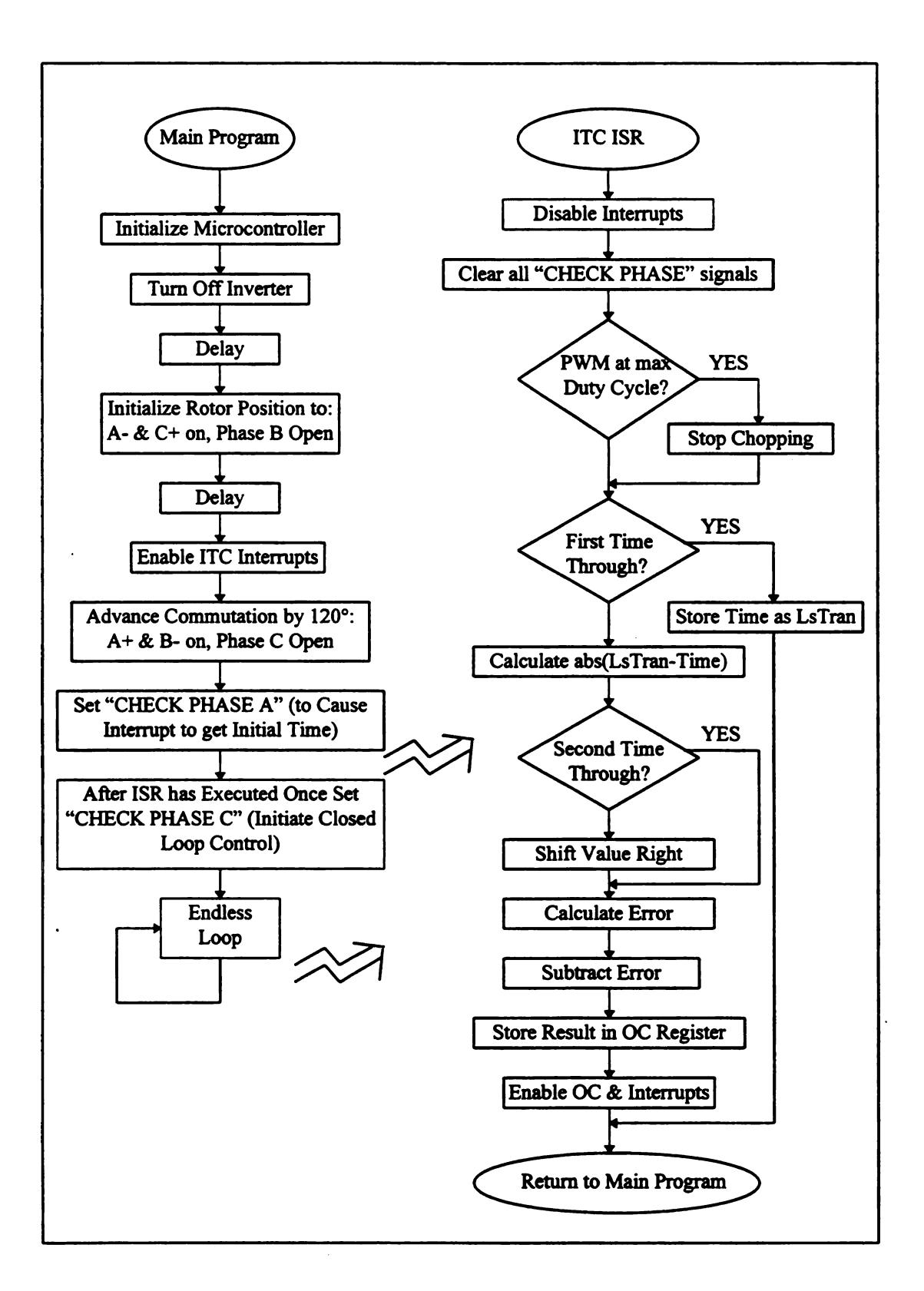


Figure 4.3 - Flow Chart of Main Program and ITC ISR

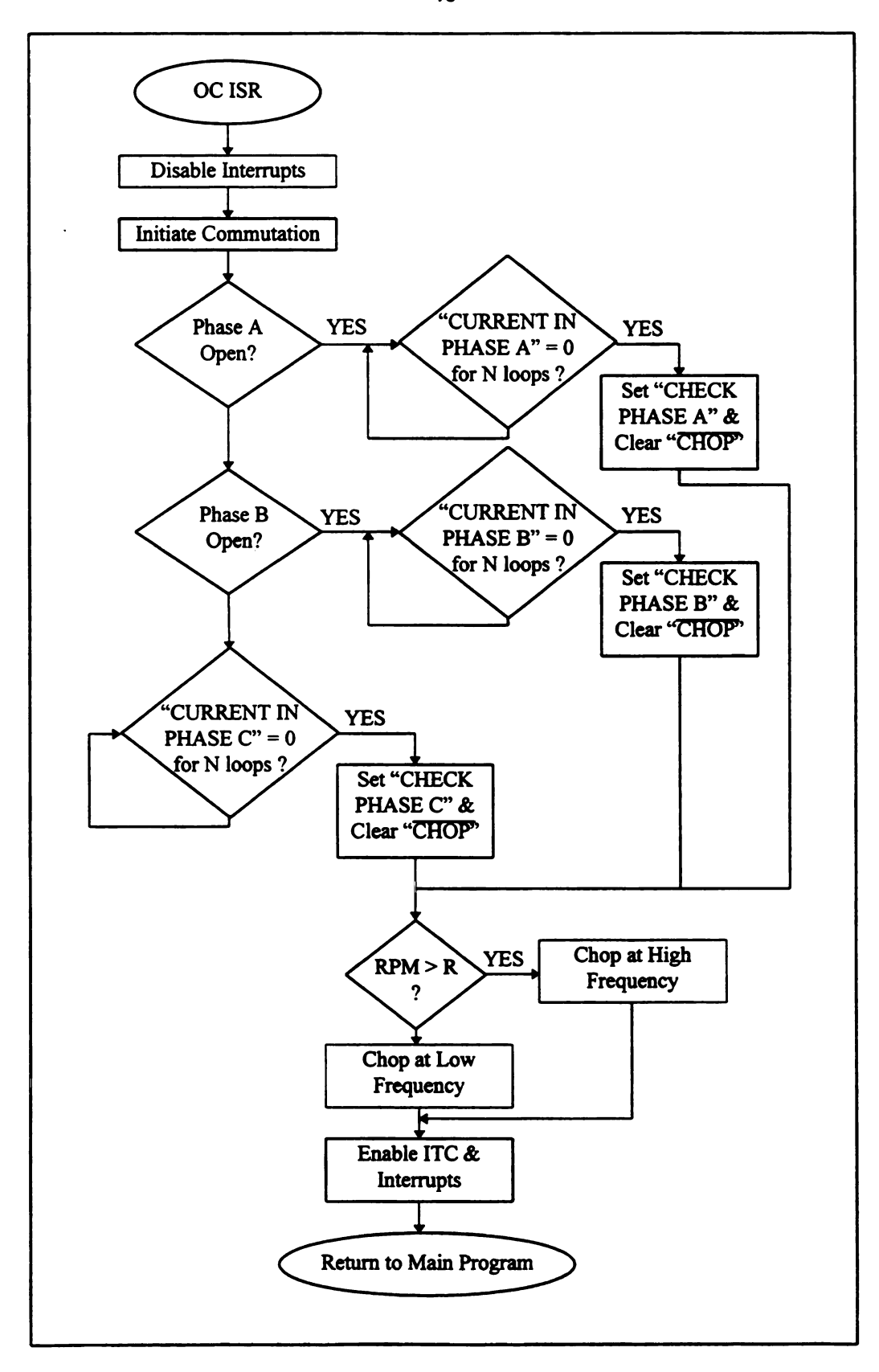


Figure 4.4 - Flow Chart of Output Compare ISR

Chapter 5

DESCRIPTION OF EXPERIMENTS AND RESULTS

Several experiments were run to determine the performance of the proposed system. This chapter is organized by experiment. Section 5.1.1 describes the tuning and validation of the detection circuit. Once the detection circuit was properly tuned, an experiment was performed to determine the actual value of K_c used in equation (2), as described in section 5.1.2. This value corresponds to the minimum speed at which the motor can spin with optimal commutation. Section 5.2 describes experiments that were performed to investigate the effects of changing the chopping scheme to lessen the amount of chopping required and to allow for higher rotor speeds as proposed earlier.

5.1 DETERMINATION OF CONSTANTS

The constant K_c , which represents the minimum induced voltage at which current can be detected in the open phase, has a theoretical value of 0.79 V. The limited sensitivity of the detection circuit results in a higher actual value for K_c . The actual value of K_c was determined through a series of experiments. The first set of experiments was designed to get the motor to operate optimally when the detection circuit is tuned to its

maximum operable sensitivity. After this was accomplished, a second set of experiments was done, in which the value of K_c was determined by trial and error using the shape of the phase currents to determine when the appropriate value was selected. Section 5.1.1 describes the first set of experiments and section 5.1.2 describes the second set.

5.1.1 TUNING AND VALIDATION OF THE DETECTION CIRCUIT

The value of K_c depends on how soon the detection circuit can detect current in the open phase. If the detection circuit is tuned to its maximum sensitivity, the value of K_c can be minimized, thus enabling the motor to operate at lower rotor speeds. The sensitivity of the detection circuit depends heavily on characteristics of the current transducers, the comparators, and the bias voltages. For a given current transducer and comparator, adjusting the bias voltages is the only way to adjust the sensitivity. Unfortunately variations in the comparators and current transducers make it necessary to individually tune the bias voltages to ensure that the detection circuit responds the same for positive and negative current in each phase. The motor will not run optimally if the current detector in one phase is more sensitive than the detector in the others, or if a detector is more sensitive to positive current than negative current.

The first step in the tuning process is to determine which comparator output provides the least sensitivity. This comparator will be the limiting factor for the detection circuit, and all of the other comparators must be tuned to match it. To determine the least

sensitive comparator we can examine the inverter input signals that are generated by the chopping selector circuit while the motor is operating with the proposed sensorless drive.

Consider the inverter input signal that controls the transistor A+ as shown in Figure 5.1. When the motor is operating properly under steady state conditions the transistor should be chopped for 60 electrical degrees and conduct for sixty electrical degrees as shown in Figure 5.1 (see also Figure 2.4). The small spikes that occur when A+ is not being chopped are the product of noise from the microcontroller and can be ignored.

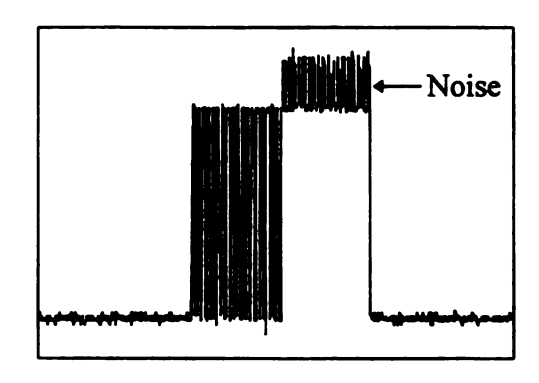


Figure 5.1 - A+ When the Motor is Operating Properly

When the transistor A+ is chopped, the transistor B- is conducting and phase C is open. The microcontroller should be examining phase C for positive current (this will indicate that the free wheeling diode is conducting). When the transistor A+ is not being chopped, and transistor C- is conducting (as in the right hand side of Figure 5.1), the microcontroller should be examining phase B for negative current. If for some reason the

comparator which detects positive current in phase C is less sensitive than the comparator that detects negative current in phase B, then the amount of time A+ is chopped will be longer than the amount of time that A+ is conducting as shown in Figure 5.2.

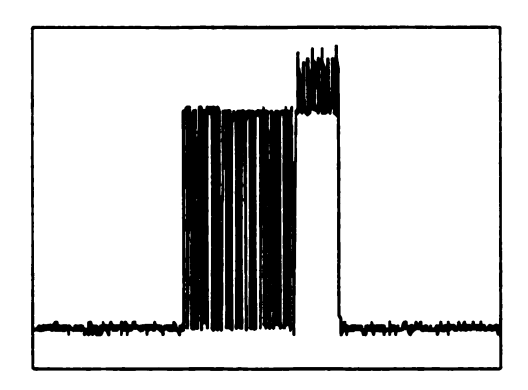


Figure 5.2 - A+ When Detection Circuit is Unbalanced

If the bias voltage of each comparator is adjusted to provide the minimum offset (the minimum offset is the offset below which the motor stalls), then the maximum amount of time that the inverter stays in any one state will correspond to the least sensitive component of the detection circuit. The rest of the comparator offset voltages can then be adjusted until the corresponding inverter state remains active for the same amount of time as the state that corresponds to the least sensitive comparator. This will ensure that the detection circuit is "balanced".

The minimum offset voltages (for balanced operation) for the comparators that detect positive current in phases A, B and C were determined to be 20.0, 15.3 and 23.8

mV respectively. The comparators that detect negative current in the motor phases were unusual because they also required positive offset voltages (negative voltages should be expected for these comparators). The maximum values for the bias voltages (for balanced operation) for the comparators that detect negative current in phases A, B, and C were determined to be 5.9, 13.7 and 6.1 mV respectively.

Figure 5.3 shows the current in phase A along with the signal generated by the portion of the detection circuit that indicates positive current in phase A. Notice that the detection circuit detects current that is almost indistinguishable from noise when viewed on an oscilloscope.

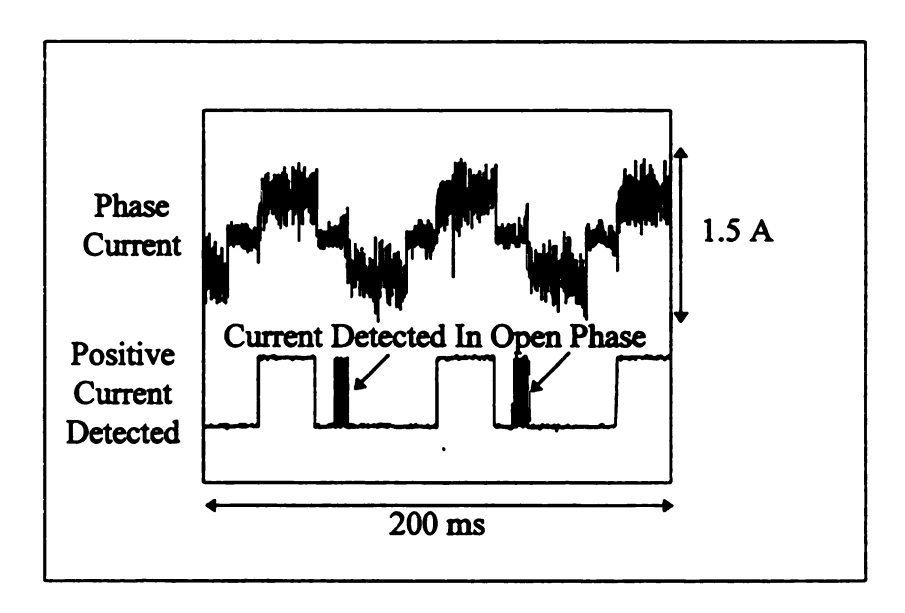


Figure 5.3 - Phase Current and Its Detection

5.1.2 DETERMINATION OF K_c

After the detection circuit is set to its maximum balanced sensitivity, the minimum value of K_c (and hence the minimum rotor speed for optimal operation) can be determined by examining the phase currents when different values of K_c are used by the microcontroller to determine the error correction term represented in equation (1). If the experimental value of K_c is too large, then the low speed error will be too large as well. This will cause the commutation to occur too soon. As a result of the early commutation, the maximum induced voltage will not yet be present in the conducting phases. Since the maximum induced voltage cannot "push back" against the applied voltage, the motor will draw a larger current. As the rotor position increases and the poles are covered by the conducting phases, the current will decrease back to its normal value. Figure 5.4 shows the phase current of the motor when the value of K_c is chosen to be too large.

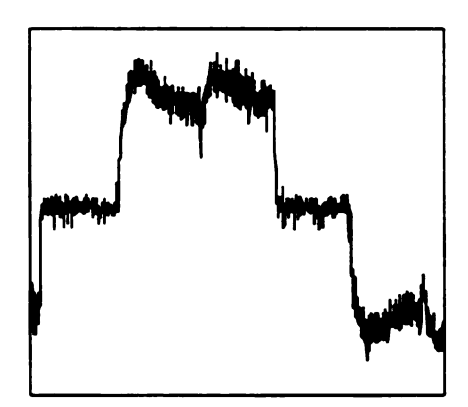


Figure 5.4 - Phase Current When K_c is too Large

If too small of a value is chosen for K_c , then the calculated commutation time will be longer than the optimal commutation time. This means that the rotor poles will pass the energized phases and the phase current will increase as shown in Figure 5.5.

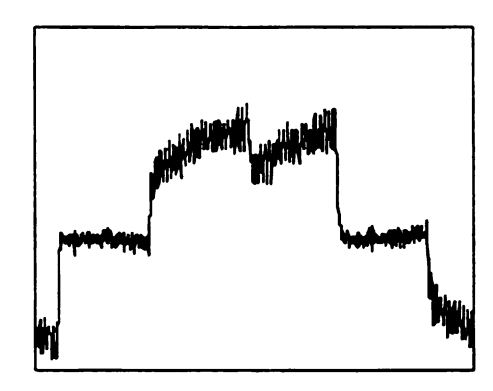


Figure 5.5 - Phase Current When $K_{\boldsymbol{c}}$ is too Small

When the proper value of K_c is chosen, the phase current should be flat (when the phase is energized) as shown in Figure 5.6.

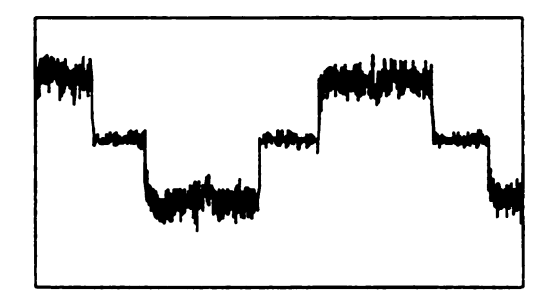


Figure 5.6 - Phase Current for Proper $\ensuremath{K_{c}}$

The actual value for K_c was determined by experiment to be 1.155 V. This corresponds to a minimum rotor speed of 55 rpm.

After selecting the proper value for K_c , the low speed error correction term represented by equation (2) was used to adjust the commutation time predicted by the method of Figure 3.5. Figure 5.7 shows how the low speed correction term adjusts the predicted commutation time. Note that the values are expressed in timer counts (1 count = 15.36 microseconds).

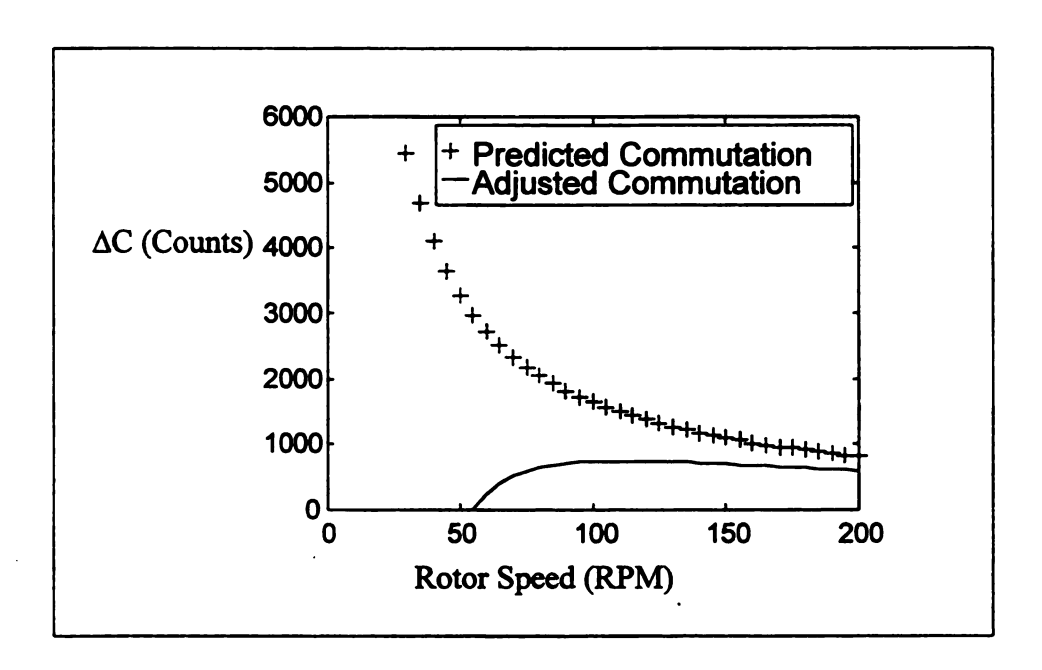


Figure 5.7 - Low Speed Error Correction

In addition to the correction factor produced by equation (2), an additional 20 counts are subtracted from the predicted commutation time to account for the delay

between the time the OC interrupt occurs and the time when the commutation actually occurs. This delay is associated with the microcontroller interrupt service time and the length of the code that is executed before the commutation in the OC ISR.

5.2 VALIDATION OF CHOPPING REDUCTION AND CHOPPING FREQUENCY ADJUSTMENT SCHEMES

As mentioned earlier, the proposed BLDC drive should stop chopping the inverter rail voltage after current is detected in the open phase, if the chopper is running at its maximum duty cycle. Attempts to validate this procedure and to quantify the actual increase in obtainable voltage as well as torque ripple were not successful for the following reasons:

It was observed that at high duty cycles, the detection circuit becomes less sensitive which results in late commutations. It was observed that at high duty cycles (97%) and low rotor speeds (less than 600 rpm) the detection of current in the open phase occurs so late that it is impossible to initiate the next commutation on time. This is true even when the commutation is commanded at the instant current is sensed in the open phase. However this is not the case if the commutation is commanded the instant that current is sensed in the open phase at high rotor speeds (greater than 600 rpm). This is fortunate since high duty cycles and low rotor speed are generally not allowed due to restrictions on phase current, however high duty cycles and high rotor speeds may be very common. Unfortunately, commanding commutation to occur as soon as current is detected in the open phase does not allow the microcontroller to stop chopping.

It may be somewhat misleading to refer to high duty cycles, since it is the amount of time which the transistor is chopped and not the percentage of conducting time which causes the detection circuit to become less sensitive. Since the TPU timer was configured so that a chopping frequency of 3 kHz was achieved by making the chopping period 34 counts long, the maximum duty cycle was 97% (33/34). If the chopping period were longer, the maximum duty cycle would increase without further loss of sensitivity by the detection circuit.

Several experiments were run to determine the maximum rotor speed when chopping at 3 kHz (a typical chopping frequency). The experiments indicated that rotor speeds above approximately 2300 rpm were difficult to achieve due to the high speed errors indicated in Figure 2.8. This is the same as the maximum speed in [4]. To allow higher speeds the microcontroller was programmed to change the chopping frequency to 6 kHz when the rotor speed exceeds approximately 700 rpm. This allowed rotor speeds well above the motor rated speed of 2500 rpm. However, decreasing the chopping period also lowers the maximum duty cycle. In this case the maximum duty cycle drops from 97% to 94%. This decrease in voltage will caused a loss in maximum rotor speed of approximately 28 rpm (from 1299 to 1271 rpm) for a 50V DC rail.

Chapter 6

FUTURE IMPROVEMENTS

The proposed system has several flaws which may limit the number of applications for which it may be used. There are two basic limitations to the proposed system. The first limitation is the system's inability to compensate for acceleration. A correction factor could have been added to account for linear accelerations as was done in the original system, however there are many applications where linear acceleration are not common. A simple method for providing compensation for all types of acceleration is proposed in section 6.1.

The second limitation is that chopping is required to detect the rotor position. The possibility of not chopping is discussed in section 6.2. Both of the proposed future improvements use the computational abilities of the microcontroller in an attempt to create a hybrid drive that uses both estimation and detection techniques to operate the motor.

6.1 DYNAMIC LOAD COMPENSATION

To account for accelerations, the microcontroller can be used to integrate the velocity of the rotor to determine position, and hence the proper commutation instant.

The linear speed-torque and torque-current relationships of the trapezoidal brushless DC motor make it easy to calculate the motor velocity if the applied voltage and current are known.

The integrator must be initialized to some known position. Since the detection of current in the open phase corresponds to a known rotor position (after taking into account the low speed errors), the detection can be used to initialize the integrator. The integrator can then indicate when the commutation should occur, thus compensating for any type of acceleration or deceleration. Figure 6.1 indicates how the microcontroller activities could correspond to the detection of current in the open phase. Notice that the integration occurs only from the time current is detected in the open phase until the next commutation. No calculations are needed after the commutation occurs until current is detected in the next open phase.

As mentioned earlier, the detection circuit becomes less sensitive at high duty cycles, and requires the commutation to be initiated as soon as current is detected in the open phase. Therefore no integration will be needed when operating at high duty cycles.

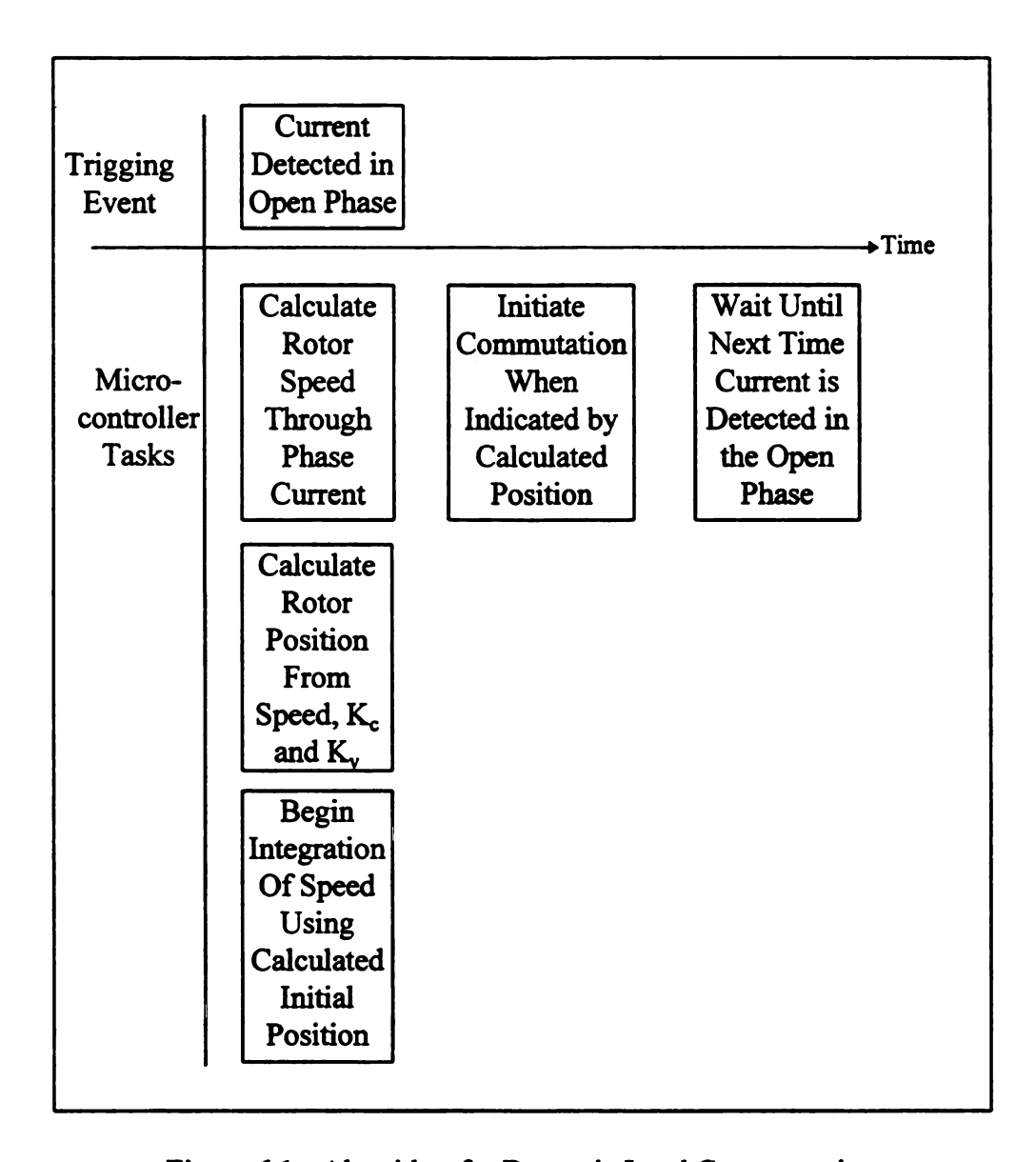


Figure 6.1 - Algorithm for Dynamic Load Compensation

6.2 ELIMINATION OF CHOPPING

There are many applications where the ability to apply the full rail voltage is desired. This is impossible for the proposed system since the full rail voltage can only be applied when there is no chopping (this is equivalent to chopping with a 100% duty cycle). Fortunately the full rail voltage is usually only commanded at high speeds due to current limitations. At high rotor speeds the induced voltage has a profound effect on the phase current. This makes it easier to calculate the rotor position via integration of the velocity for long periods of time.

It is proposed that if the duty cycle is commanded to 100%, the last occurrence of current in the open phase (from before the duty cycle was 100%) should initiate and initialize integration of the velocity (as described above), and that the integration continue until a lower duty cycle is commanded.

For example, assume that the motor is operating at a low duty cycle, and integrating the phase current as described earlier. The integration was initialized the last time current was detected in the open phase. If the duty cycle is then commanded to 100%, instead of ceasing the integration after the commutation, simply continue until the duty cycle is lowered and current can be detected in the open phase again. Since the induced voltage is large, the integration should provide a sufficiently accurate estimate of the rotor speed. This is a calculation intensive procedure that represents the transition from a sensorless detection drive to a sensorless estimation based drive.

Chapter 7

CONCLUSIONS AND COMMENTS

The experiments of Chapter 5 prove that the proposed sensorless drive allows the motor to operate at a wider speed range than the original system proposed by Ogasawara and Akagi. Experiments show that the motor can operate at speeds from 55 to over 2500 rpm efficiently. The proposed drive should be more efficient than the drive in [4] since it provides much more accurate error correction at low rotor speeds. The proposed system corrects for low speed error down to 55 rpm, whereas the original system initiated commutation as soon as current is detected in the open phase at all speeds below 500 rpm.

The proposed system can achieve a maximum rotor speed that is more than 200 rpm faster than the original system due to the implementation of a variable chopping frequency. However the increase in chopping frequency is generally accompanied by a decrease in the maximum applicable voltage since the DC rail voltage must be chopped for some fixed minimum amount of time.

The minimum speed of the motor with the proposed system is approximately 10 rpm higher than that of the original system. However this should be expected since the motor used in [4] had a higher voltage constant (K_v) and a lower conducting voltage drop

across the free-wheeling diodes and power transistors of the inverter (K_c) . The theoretical minimum operating speed of the motor used with the proposed drive is approximately 36 rpm whereas the theoretical minimum operating speed of the motor used with the original system was 22 rpm. The proposed system is able to come much closer to its theoretically minimum speed than the original system. This indicates that the use of current transducers and the proposed detection circuit is equally if not more sensitive than the detection circuit of the original system (when the duty cycle is not too high).

Attempts to reduce the amount of time that the rail voltage was chopped were not successful due to an unexpected decrease in the sensitivity of the detection circuit at high duty cycles. This loss of sensitivity, however, does not interfere with the motor's ability to achieve high speeds, but makes the drive less efficient when operating at low speeds.

It should be noted that speed and torque control were not mentioned in this thesis.

The goal of the proposed drive was to allow the motor to operate properly, no matter what the commanded speed or torque. This means that any speed or torque control may be implemented independently of the commutation scheme.

In summary, the two main weaknesses of the proposed drive are the need for chopping, and the inability to compensate for a dynamic load. These weakness may be overcome using the modifications suggested in the previous chapter. In nearly all other respects the proposed drive obtains superior performance when compared to the original system.

APPENDIX A

- * This Program is intended to drive a brusless D.C.
- * motor without rotor position sensors.
- * The software requires very specific hardware to
- * interface with the drive

org \$4000

SYNCR		EQU \$FFFA04	CPU CLOCK SYN. CONTROL	
REG				
TPUMCR	EQU	\$FFFE00	TPU Module Control Register	
TICR	EQU	\$FFFE08	TPU Interrupt Enable Register	
CIER	EQU	\$FFFE0A	TPU Channel Interrupt Enable Reg	
CISR	EQU	\$FFFE20	TPU Channel Intrpt. Status Reg	
CFSR3	EQU	\$FFFE12	TPU Channel Function Select Reg	
HSQR1	EQU	\$FFFE16	TPU Host Sequence Register 1	
CH0PAR0	EQU	\$FFFF00	TPU Channel 0 Parameter 0 Reg	
CH0PAR2	EQU	\$FFFF04	TPU Channel 0 Parameter 2 Reg	
CH0PAR3	EQU	\$FFFF06	" " 3	
CH1PAR0	EQU	\$FFFF10	TPU Channel 1 Parameter 0 Reg	
CH1PAR1	EQU	\$FFFF12	5	
CH1PAR2	EQU	\$FFFF14	TPU Channel 1 Parameter 2 Reg	
FINTRAN	EQU	\$FFFF18	_	
CH2PAR0	EQU	\$FFFF20	TPU Channel 2 Parameter 0 Reg	
CH2PAR1	EQU	\$FFFF22	100 0 0 0 0 0 0 0 0 0 0 0 0 0 0 0 0 0 0	
CH2PAR2	EQU	\$FFFF24	TPU Channel 2 Parameter 2 Reg	
CH2PAR3	EQU	\$FFFF26		
HSRR0	EQU	\$FFFE18		
HSRR1	EQU	\$FFFE1A	TPU Host Service Request Reg 1	
CPR0	EQU	\$FFFE1C	The field service reduces real	
CPR1	EQU	\$FFFE1E	TPU Channel Priority Reg 1	
PEPAR	EQU	\$FFFA17	PORT E PIN ASSIGNMENT REG.	
DDRE	EQU	\$FFFA15	PORT E DATA DIRECTION REG.	
PORTE	EQU	\$FFFA13	PORT E DATA DIRECTION REG.	
IONIL	ŁQU	DITI'MIS	I OKI L DAIA KEOISIEK	

******Logic Signals For Inverter, Flags & Variables*****

STATO dc.w %0000011010011010 First Inverter state A+ and B- on Coff

A+A-B+B-C+C-

STAT1	dc.w	%0000011010101001	A+.C- Boff
STAT2	dc.w	%0000101001101001	B+,C- Aoff
STAT3	dc.w	%0000100101101010	B+,A- Coff
STAT4	dc.w	%0000100110100110	C+,A- Boff
STAT5	dc.w	%0000101010010110	C+,B- Aoff
STATZ	dc.w	%0000101010101010	All OFF
STATE	dc.b	\$ 0	STATE OF INVERTER
FirsTIM	dc.b	0	Flag to get initial time
LsTran	dc.w	0	Last time spikes occured
SndTIM	dc.b	0	Second time through ISR1 (first comm)
ChopMode	dc.b	0	Chopping Freq $(0 = Low, 1 = HI)$
*******	*****	*****	
		rupt Vectors********	*****
org \$		61000 4	TRUE CLASS AND CONTRACTOR AND
CH1VEC		\$10004	TPU Ch 1 Interrupt Service Routine location
CH2VEC		\$10204	TPU Ch 2 "
	3000	nitialization *******	
move	e.w	#\$FFFF,D2	
move	e.w	#\$CF80,SYNCR	SET SYSTEM CLOCK TO 16MHz
		,	
* ****	***SET	UP PORT E AS INPU	
move	e.b	#\$00,PEPAR Set Por	
move	e.b	#\$00,DDRE Set Por	rt E to INPUT
* ****	*****	Γ UP TPU MAIN REG	ICTED C********
		#\$608E,TPUMCR	PRESCALE TCR1 BY 8 SET IARB TO \$E
move	E.W	#\$006E, I PUNICK	PRESCALE ICKI BI 6 SEI IARB 10 JE
move	e.w	#\$0640,TICR	TPU INTRP LEV. 6 VECTOR AT 4*40
move	e.w	#\$8EA9,CFSR3	Ch 1 = ITC Ch0=PWM ch2 =OC ch3=DIO
move		#\$0888,CFSR3-2	Ch 4,5 = DIO, CH6 = No Chop
move		#\$8888,CFSR3-4	Ch 8,9,10,11 = DIO
move		#\$0088,CFSR3-6	ch 12,13 = DIO
		•	•
* ****	**SET U	JP DIO CHANNELS (ENABLES and Inverter)*****
		201010101010202	
mav	ອ ນ <i>ນ</i> #ບ/∧ໃ	3010101010000000 HS	RR1 Set FNARI F A R C Low (disable)

move.w #%0010101010000000,HSRR1 Set ENABLE A,B,C Low (disable)
Allow Chopping

#%00111111111000000,CPR1

move.w

bra

Set CH 3-6 & 8-13

to High Priority #%0000111111111111,CPR0 move.w **********SET UP CHANNEL 1 (INPUT)******* #\$0004,HSQR1 Ch1 One Continuous mode (no links) ori.w #\$0007,CH1PAR0 Ch1 Detect Either edge move.w No Start Link or Link chan ent or BA #\$000E,CH1PAR1 move.w Max Count = 1 (count 1 transition)#\$0001,CH1PAR2 move.w #\$0004,HSRR1 Initialize ch1 (ITC) move.w #\$000C,CPR1 Set CH1 high priority ori.w clr.w D₀ WAIT1 move.w HSRR1,D0 WAIT TO MAKE SURE ITC INITIALIZTION andi.w #\$0F,D0 IS COMPLETE bne WAIT1 *************end of chl setup*********** SET CHANNEL ZERO #\$0091,CH0PAR0 move.w #\$1C,CH0PAR2 **HIGH TIME (COUNTS)** move.w move.w #\$22,CH0PAR3 PERIOD (COUNTS) #\$0002,HSRR1 Initialize ch0 (PWM) move.w ori.w #\$0003,CPR1 Set Ch0 high priority clr.w D0WAIT0 move.w HSRR1,D0 WAIT TO MAKE SURE PWM INITIALIZTION andi.w #\$0F,D0 IS COMPLETE bne WAIT0 Turn off all phases and wait about 6 sec. STATZ,A0 lea (A0),D0move.w D0,HSRR0 move.w clr.l D₀ delay addi.l #1,D0 cmpi.l #\$1FFFFF,D0 beq start delay

****** Set duty cycle to max safe voltage start move.w #\$15,CH0PAR2 High time (counts)

****** Initialize rotor position

clr.w D0

lea STAT3,A0 move.w (A0)+,D0

move.w D0,HSRR0

****** Wait for rotor to move to initial position

clr.l D0

INIPOS addi.l #1,D0

cmpi.l #\$FFFF,D0 delay time can be adjusted

bmi INIPOS

****** Start first commutation (state 5)

lea STAT5,A0 move.w (A0)+,D0

move.w D0,HSRR0

******* Get Initial Time (using Channel 1)

move.w #\$0002,CIER ENABLE CHANNEL 1 INTERRUPTS

andi.w #\$F0FF,sr ENABLE INTERRUPS

ori.w #\$0500,sr

move.w #\$540,HSRR1 set all enables to trigger intrpt

that gets initial time

getTIM move.b FirsTIM,D0 Wait until Initail Time is stored

beq getTIM

*****	**	Check for no current in open phase (A) and set enable					
		btst.b	- · · · · · · · · · · · · · · · · · · ·		if commutation is done (no current in		
		bne	NotOF			open phase) then	
		move.	w #\$40,H	SRR1		set ENABLEA	
****	*****		******		******	*****	
*****	**		e Closed Loop (*****		
****	*****	*****				******	
	move.		•	,		ANNEL 1 INTERRUPTS	
	andi.w		#\$F0FF,sr	ENA	ENABLE INTERRUPS		
	ori.w		#\$0500,sr		"		
****	*****	*****	*****	*****	*****	******	
****	 ***	N		*****	****	****	
****	*****		PROGRAM	*****	*****	*****	
outloo		bra	outloop				
Outloo	P	ora	outloop				
****	*****	*****	******	*****	*****	******	
****	****	Interru	ot Service Routi	nes ****	*****	****	
****			•		*****	******	
****	*****	**Inter	upt Service Rou	utine For Cha	nnel 1**	*****	
	org \$1		•				
	andi.w	7	#\$FFFD,CIER	DISA	ABLE CH	HANNEL 1 INTERRUPTS	
move.w		CISR,D6 · Clear Cl		Channel 1 IRQ			
	andi.w	7	#\$FFFD,CISR				
	move.	w	#%000010101	000000,HS !	RR1	TURN OFF ENABLEA,B,C	
*	Stop C	Choppin	g if at max duty	•			
	move.	w	CH0PAR3,D5				
	sub.w		CH0PAR2,D5				
	cmpi.v	v	#7,D5				
	bhi		CHOP				
	move.	w	#%000100000	0000000,HS	RR1	Stop Chopping	
				•			

СНОР	move.b bne move.w move.b bra	FirsTIM,D0 NotFrst FINTRAN,Ls' #\$FF,FirsTIM END2		
NotFrst	move.w move.w	FINTRAN,D3 LsTran,D4 D3,D7	SAVE COUNTER VALUES	
	cmp.w bhi	D3,D4 ROLLOVER		
	sub.w bra	D4,D3 CHKsnd	Calculate offset time	
ROLLOVER	clr.l	D0		
	move.w	#\$FFFF,D0		
	sub.w	D4,D0		
	add.w	D0,D3		
CHKsnd	move.b	SndTIM,D0		
	bne	NotScnd		
	move.b	#\$FF,SndTIM		
	bra	SETINT		
NotScnd	move.w	D3,D2	STOR FOR USE IN OC ISR	
	lsr.w	#1,D3		
*	•	***** Adjust for errors *****		
	clr.l	D0		
	clr.l	D1		
	move.w	D3,D1		
	mulu.w	D3,D1		
	mulu.l	•	theoretical min)	
	lsr.l	#8,D1	shift to divide	
	lsr.l	#8,D1	by 2^-16	
	sub.w	D1,D3		
*	sub.w	#20,D3	Use this line	
*	clr.w	D3	at max duty cycle	
*			only!	
	bpl	SETINT		
	clr.w	D3		

FINTRAN.LsTran SETINT move.w #\$0083,CH2PAR0 SET CHANNEL TWO move.w move.w D3,CH2PAR1 OFFSET (WRITTEN BY CH1 ISR) move.w #\$0018,CH2PAR2 REFERENCE ADDRESS FROM CH1 INPUT TIME #\$0000,HSQR1 ori.w Schedule Interrupt #\$0010,HSRR1 Init move.w #\$0030,CPR1 Set Ch2 high priority ori.w clr.w D0WAIT2 move.w HSRR1,D0 WAIT TO MAKE SURE OC INITIALIZTION andi.w #\$0030,D0 IS COMPLETE WAIT2 bne ori.w #\$0004,CIER **Enable Channel 2 Interrupts** *********End of Channel 1 ISR************** org \$10204 **DISABLE CHANNEL 2 INTERRUPTS** andi.w #\$FFFB,CIER CISR.D6 Clear Channel 2 IRQ move.w #\$FFFB,CISR andi.w cmpa.l #STAT5,A0 **NXTREV** bhi bra COMM NXTREV lea STATO,A0 move.b #00,STATE COMM (A0)+,D0move.w D0,HSRR0 move.w ***** Wait For Commutation to complete ******* D0 clr.l

move beq cmpi. beq bls cmpi. beq bls	COFF b #2,D0 AOFF BOFF	open	hich phase should be
AOFF	move.b	#60, D 5	
AOFF1	btst.b	#3,PORTE	if commutation is done (no current in
	bne	AOFF	open phase) then
	subi.b	#1,D5	
	bne	AOFF1	
	move.w	#\$2040,HSRR1	set ENABLEA Start Chopping
	bra	END2	
BOFF	move.b	#60,D5	
BOFF1	btst.b	#2,PORTE	
	bne	BOFF	
	subi.b	#1,D5	
	bne	BOFF1	
	move.w	#\$2100,HSRR1	set ENABLEB Start Chopping
	bra	END2	
COFF	move.b	#60,D5	
COFF1	btst.b	#1,PORTE	
	bne	COFF #1 D5	
	subi.b	#1,D5	
	bne move.w	COFF1 #\$2400,HSRR1	
	bra	#32400,113RK1 END2	set ENABLEC Start Chopping
	01a	LINDZ	Set LIVADELE Start Chopping
* ****	**** Adjust Ch	opping Frequency to	account for speed *****
END2 clr.l	D0	·	
move	.b Chop	Mode,D0	
bne	HiMo	ode	
cmpi.	w #446,	D2	Check to see if rpm > 700
bhi	Cont		

CH0PAR2,D0

#8,D0 #7,D0

move.w

lsl.l lsl.l

	move.l D		#\$11,D0 D0,CH0PAR2 #1,ChopMode		if rmp > 700 go to hi mode	
HiMoo	de	cmpi.v bls move. lsl.l lsl.l move. move. move.	w W I	#446,D2 Cont CH0PAR2,D0 #8,D0 #8,D0 #1,D0 #\$22,D0 D0,CH0PAR2 #0,ChopMode	if rpm < 700 go to low mode	
Cont		addi.b ori.w rte		#1,STATE #\$0002,CIER	Enable Channel 1 Interrupts	
**************end of ch2 ISR*****************						

BIBLIOGRAPHY

- [1] G. C. Young and R. Kiefer, "Electronically Commutated Motor for Driving a Compressor," United States Patent, Patent Number 5,491,978, February 20, 1996
- [2] Nobuyuki Matsui, "Sensorless PM Brushless DC Motor Drives," IEEE Transactions on Industrial Electronics, vol. 43, pp. 300-308, April 1996
- [3] K Iizuka, H. Uzuhashi, M. Kano, T. Endo and K. Mohri, "Microcomputer Control for Sensorless Brushless Motor," IEEE Transactions on Industry Applications, vol. IA-21, pp. 595-601, June 1985.
- [4] Satoshi Ogasawara and Hirofumi Akagi, "An Approach to Position Sensorless Drive for Brushless dc Motors," IEEE Transactions on Industry Applications, vol. 27, pp. 928-933, September 1991

MICHIGAN STATE UNIV. LIBRARIES